

Unfolding Polycube Trees with Constant Refinement*

Mirela Damian[†] Robin Flatland[‡]

Abstract

We show that every polycube tree can be unfolded with a 4×4 refinement of the grid faces. This is the first constant refinement unfolding result for polycube trees that are not required to be well-separated.

1 Introduction

An *unfolding* of a polyhedron is obtained by cutting its surface in such a way that it can be flattened in the plane as a simple non-overlapping polygon called a *net*. An *edge unfolding* allows only cuts along the polyhedron's edges, while a *general unfolding* allows cuts anywhere on the surface. Edge cuts alone are not sufficient to guarantee an unfolding for non-convex polyhedra [BDE⁺03, BDD⁺98], however it is unknown whether all non-convex polyhedra have a general unfolding. In contrast, all convex polyhedra have a general unfolding [DO07, Sec. 24.1.1], but it is unknown whether they all have an edge unfolding [DO07, Ch. 22].

Prior work on unfolding algorithms for non-convex objects has focused on orthogonal polyhedra. This class consists of polyhedra whose edges and faces all meet at right angles. Because not all orthogonal polyhedra have edge unfoldings [BDD⁺98], the unfolding algorithms typically use additional non-edge cuts that follow one of two models. In the *grid unfolding model*, the surface is subdivided into rectangular *grid faces* by adding edges where axis-perpendicular planes through each vertex intersect the surface, and cuts along these added edges are also allowed. In the *grid refinement model*, each grid face under the grid unfolding model is further subdivided by an $(a \times b)$ orthogonal grid, for some positive integers $a, b \geq 1$, and cuts are also allowed along any of these grid lines.

A series of algorithms have been developed for unfolding arbitrary genus-0 orthogonal polyhedra, with each successive algorithm requiring less grid refinement. The first such algorithm [DFO07] required an exponential amount of grid refinement. This was reduced to quadratic refinement in [DDF14], and then to linear in [CY15]. These ideas were further extended in [DDFO17] to unfold arbitrary genus-2 orthogonal polyhedra with linear refinement.

The only unfolding algorithms for orthogonal polyhedra that use sublinear refinement are for specialized orthogonal shape classes. For example, there exist algorithms for unfolding orthostacks using 1×2 refinement [BDD⁺98] and Manhattan Towers using 4×5 refinement [DFO05]. There also exist unfolding algorithms for several classes of polyhedra composed of rectangular boxes. For example, orthotubes [BDD⁺98] and one layer block structures [LPW14] built of unit cubes with an arbitrary number of unit holes can both be unfolded with cuts restricted to the box edges. Our focus here is on a class of orthogonal polyhedra known as polycube trees. A *polycube tree* \mathcal{O} is composed of axis-aligned unit cubes (boxes) glued face to face, whose surface is a 2-manifold and whose dual graph \mathcal{T} is a tree. (See Figure 1a for an example.) In the grid unfolding model, cuts are allowed along any of the cube edges. Each node in \mathcal{T} is a box in \mathcal{O} and two nodes are connected by an edge if the corresponding boxes are adjacent in \mathcal{O} (i.e., if they share a face). In this paper we will use the terms *box* and *node* interchangeably. The *degree* of a box $b \in \mathcal{O}$ is defined as the degree of its corresponding node in the dual tree \mathcal{T} . We select any node of degree one to be the *root* of \mathcal{T} .

In a polycube tree, each box can be classified as either a *leaf*, a *connector*, or a *junction*. A leaf is a box of degree one; a connector is a box of degree two whose two adjacent boxes are attached on opposite faces; all other boxes are junctions.

*Partial results for polycube trees (previously called *orthotrees*) of degree 3 or less have appeared in [DF18].

[†]Department of Computer Science, Villanova University, Villanova, PA, mirela.damian@villanova.edu

[‡]Department of Computer Science, Siena College, Loudonville, NY, flatland@siena.edu

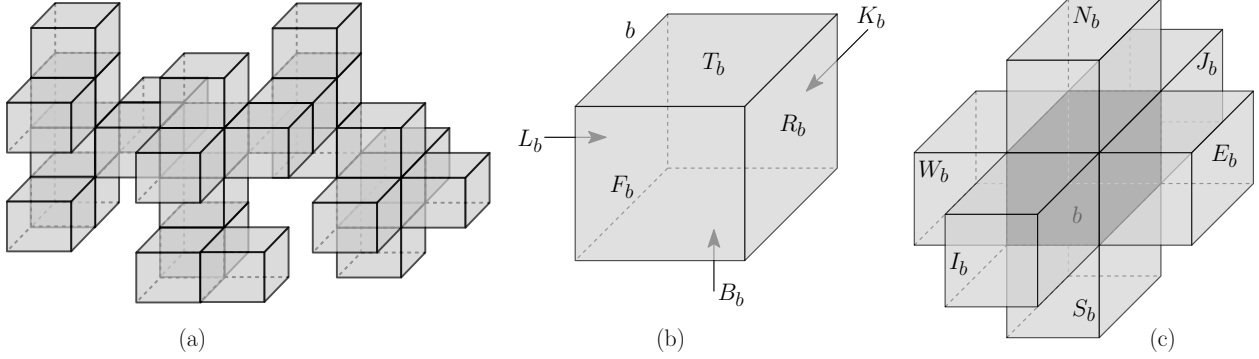


Figure 1: (a) A simple polycube tree example. Notation for: (b) b 's faces (c) b 's neighbors.

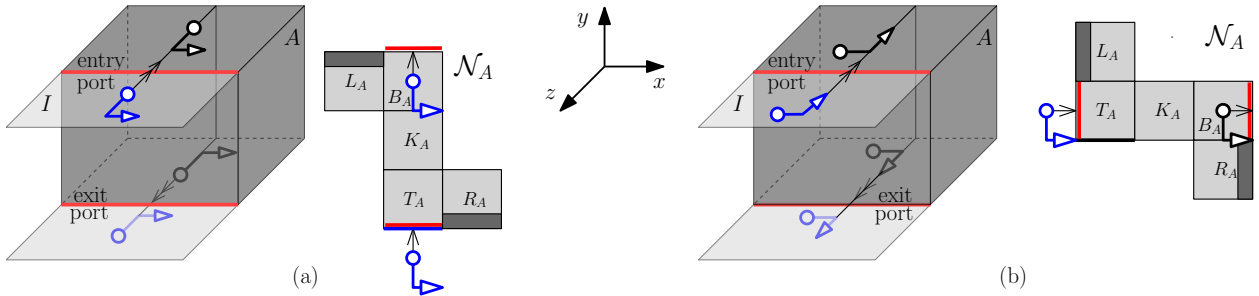


Figure 2: (a) HEAD-first and (b) HAND-first unfolding of leaf box; dark-shaded pieces can be removed without disconnecting the nets.

Because polycube trees are orthogonal polyhedra, they can be unfolded using the general algorithm in [CY15] with linear refinement. Algorithms for unfolding polycube trees using less than linear refinement have been limited to polycube trees that are *well-separated*, meaning that no two junction boxes are adjacent. In [DFMO05], the authors provide an algorithm for grid unfolding well-separated polycube trees. Recent work in [HCY17] shows that the related class of well-separated orthographs (which allow arbitrary genus) can be unfolded with a 2×1 refinement.

In this paper we provide an algorithm for unfolding all polycube trees using a 4×4 refinement of the cube faces. For each box b in \mathcal{T} , the algorithm unfolds b and the boxes in the subtree rooted at b recursively. Intuitively, the algorithm unfolds surface pieces of b along a carefully constructed path. When the path reaches a child box of b , the child is recursively unfolded and then the path continues on b again to the next child (if there is one). The unfolding of b and its subtree is contained within a rectangular region having two staircase-like bites taken out of it. This is the first sublinear refinement unfolding result for the class of all polycube trees, regardless of whether they are well-separated or not.

2 Terminology

For any box $b \in \mathcal{O}$, R_b and L_b are the *right* and *left* faces of b (orthogonal to the x -axis); F_b and K_b are the *front* and *back* faces of b (orthogonal to the z -axis); and T_b and B_b are the *top* and *bottom* faces of b (orthogonal to the y -axis). See Figure 1b. We use a different notation for boxes adjacent to b , to clearly distinguish them from faces: E_b and W_b are the *east* and *west* neighbors of b (adjacent to R_b and L_b , resp.); N_b and S_b are the *north* and *south* neighbors of b (adjacent to T_b and B_b , resp.); and I_b and J_b are the *front* and *back* neighbors of b (adjacent to F_b and K_b , resp.). See Figure 1c. We omit the subscript whenever the box b is clear from the context. We use combined notations to refer to the east neighbor of N as *NE*, the back neighbor of *NE* as *NEJ*, and so on.

If a face of a box $b \in \mathcal{O}$ is also a face of \mathcal{O} , we call it an *open face*; otherwise, we call it a *closed face*.

On the closed face shared by b with its parent box in \mathcal{T} , we identify a pair of opposite edges, one called the *entry port* and the other called the *exit port* (shown in red and labeled in Figure 2). The unfolding of b is determined by an *unfolding path* that starts on b near b 's entry port, recursively visits all boxes in the subtree $\mathcal{T}_b \subseteq \mathcal{T}$ rooted at b , and ends on b near b 's exit port. We denote by \mathcal{N}_b the unfolding net produced by a recursive unfolding of b . For simplicity, we will sometimes omit the word “recursive” when referring to a recursive unfolding of a box b and simply call it an *unfolding of b* , with the understanding that all boxes in \mathcal{T}_b get unfolded during the process.

To make it easier to visualize the unfolding path, we use an *L-shaped guide* (or simply *L-guide*) with two orthogonal pointers, namely a *HAND pointer* and a *HEAD pointer*. (See Figure 2, where the HEAD and the HAND pointers are represented by the circle and the arrow, respectively.) With very few exceptions, the unfolding path extends in the direction of one of the two pointers. Whenever the unfolding path follows the direction of the HAND, we say that it extends *HAND-first*; otherwise, it extends *HEAD-first*. Surface pieces traversed in the direction of the HAND (HEAD) will flatten out horizontally (vertically) in the plane.

As a simple example, consider the unfolding of a leaf box A from Figure 2a. The *L-guide* is shown positioned on top of A 's parent box I at the entry port. The unfolding path extends HEAD-first across the top, back, and bottom faces of A , and ends on the bottom of A at the exit port. The resulting unfolding net \mathcal{N}_A consists of A 's open faces T_A, K_A, B_A, L_A , and R_A . In all unfolding illustrations, the outer surface of \mathcal{O} is shown. When describing and illustrating the unfolding of a box A , we will assume without loss of generality that the box is in *standard position* (as in Figure 2a), with its parent I_A attached to its front face F_A and its entry (exit) port on the top (bottom) edge of F_A .

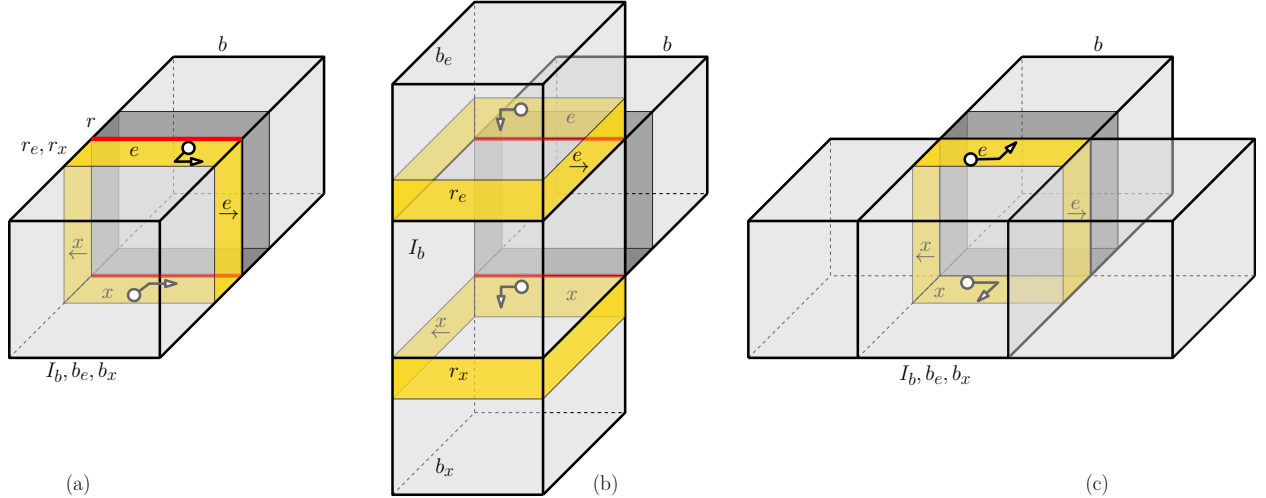


Figure 3: Box b in standard position with parent I_b and ring r (a) entry and exit boxes b_e, b_x coincide with parent I_b ; entry ring r_e coincides with exit ring r_x ; entry ring face $e \in r_e$ is the top and its successor $\xrightarrow{e} \in r_e$ is the right face of r_e ; exit ring face $x \in r_x$ is the bottom and its predecessor $\xleftarrow{x} \in r_x$ is the left face of r_x (b) entry box b_e with entry ring r_e and entry face e lies north of I_b ; exit box b_x with exit ring r_x and exit face x lie south of I_b ; \xrightarrow{e} is the successor of e on the entry ring r_e , and \xleftarrow{x} is the predecessor of x on the exit ring r_x (c) \xrightarrow{e} and \xleftarrow{x} are closed (e and x are always open, by definition).

The *ring* r of a box b includes all the points on the surface of b (not necessarily on the surface of \mathcal{O}) that are within distance $1/4$ of the closed face shared with b 's parent. Thus, r consists of four $1/4 \times 1$ rectangular pieces (which we call *ring faces*) connected in a cycle. (See Figure 3a, where r is the shaded band on b 's surface wrapping around b 's front face; box b is shown in standard position, so its parent I_b attaches to b 's front face.) The *entry box* b_e of b is the box containing the open face in $\mathcal{T} \setminus \mathcal{T}_b$ adjacent to b 's entry port. Note that b_e may be b 's parent (as in Figure 3a), but this is not necessary (see Figure 3b, where b_e is the box on top of b 's parent I_b).

The *entry ring* r_e of b includes all points of b_e that are within distance $1/4$ of the closed face of b_e adjacent to b 's entry port. (Refer to Figure 3.) The face e of r_e adjacent to b 's entry port is the *entry ring face*. Similarly, the *exit box* b_x of b is the box containing the open face in $\mathcal{T} \setminus \mathcal{T}_b$ adjacent to b 's exit port. Note that

b_x may be b 's parent (as in Figure 3a), but this is not necessary (see Figure 3b, where b_x is the box south of b 's parent I_b). The *exit ring* r_x of b includes all points of b_x that are within distance $1/4$ of the closed face of b_x adjacent to b 's exit port. The face x of r_x adjacent to b 's exit port is the *exit ring face*. Note that both e and x are *open* ring faces (by definition). When unclear from context, we will use subscripts (i.e., e_b and x_b) to specify the entry and exit faces of a particular box b .

In a HEAD-first unfolding of a box b , the *L-guide* begins on the entry ring face e with the HEAD pointing toward the entry port, and it ends on the exit ring face x with the HEAD pointing away from the exit port; the HAND has the same orientation at the start and end of the unfolding. (See Figures 2a, 3a.) Similarly, in a HAND-first unfolding, the *L-guide* begins on the entry ring face e with the HAND pointing toward the entry port, and it ends on the exit ring face x with the HAND pointing away from the exit port; the HEAD has the same orientation at the start and end of the unfolding. (See Figures 2b, 3b.) In standard position, the HAND in a HEAD-first unfolding will point either east or west. If it points east (west) we say that the unfolding is a HAND-east (west), HEAD-first unfolding. Similarly, in a HAND-first unfolding, the HEAD will either point east or west. If it points east (west), we say the unfolding is a HEAD-east (west), HAND-first unfolding.

In a HEAD-first (HAND-first) unfolding of b with entry ring face e , \xrightarrow{e} is the ring face of r_e encountered immediately after e when cycling around r_e in the direction pointed to by the HAND (HEAD) of the *L-guide* as positioned on e at the start of b 's unfolding. Similarly, in a HEAD-first (HAND-first) unfolding of b with exit ring face x , \xleftarrow{x} is the ring face of r_x encountered just before x when cycling around r_x in the direction pointed to by the HAND (HEAD) of the *L-guide* as positioned on x at the end of b 's unfolding path. Figure 3 shows \xrightarrow{e} and \xleftarrow{x} labeled. Note that, although e and x are open ring faces by definition, \xrightarrow{e} and \xleftarrow{x} may be closed (see Figure 3c for an example).

3 Inductive Regions

Let $b \in \mathcal{T}$ be an box to be unfolded recursively.

Definition 1. A HEAD-first *inductive region* for b is a rectangle at least three units wide and three units tall, with two staircase bites taken out of the lower left and upper right corners, as shown in Figure 4a. The *entry* (*exit*) port of the inductive region is the lower left (upper right) horizontal segment that lies strictly inside the bounding box of the region. If b is not a leaf, the unit cells labeled \mathcal{E}_b and \mathcal{X}_b in Figure 4a are conditionally included in the inductive region as follows:

- If the successor \xrightarrow{e} of the entry ring face e is closed, then \mathcal{E}_b is included as part of the inductive region, otherwise, \mathcal{E}_b is not part of the inductive region. In the latter case, we refer to the unit segment right of the entry port as the *entry port extension*.
- If the predecessor \xleftarrow{x} of the exit ring face x is closed, then \mathcal{X}_b is included as part of the inductive region, otherwise, \mathcal{X}_b is not part of the inductive region. In the latter case, we refer to the unit segment left of the exit port as the *exit port extension*.

See Figure 5 for a few examples. A HEAD-first unfolding of b produces a net \mathcal{N}_b that fits within the HEAD-first inductive region and whose entry (exit) port aligns to the left (right) with the entry (exit) port of the inductive region.

A HAND-first *inductive region* for b is an orthogonally convex polygon shaped as in Figure 4b. Its shape is isometric to that of a HEAD-first inductive region, and one can be obtained from the other through a clockwise 90° -rotation, followed by a vertical reflection. The unit cells \mathcal{E}_b and \mathcal{X}_b in Figure 4b are conditionally included in the inductive region according to the rules stated in Definition 1.

Lemma 2. Let b be an arbitrary box in \mathcal{O} , and let d be the box corresponding to b in a horizontal reflection of \mathcal{O} . Let \mathcal{N}_d be the unfolding net produced by a HEAD-first unfolding of d . If \mathcal{N}_d is rotated counterclockwise by 90° and then reflected horizontally, then the result is a HAND-first unfolding of b .

Proof. First note that, when applied to the L-guide, the combined (90° -rotation, reflection) transformation switches the HEAD and HAND positions. This implies that the successor \xrightarrow{e} of d 's entry ring face is the same

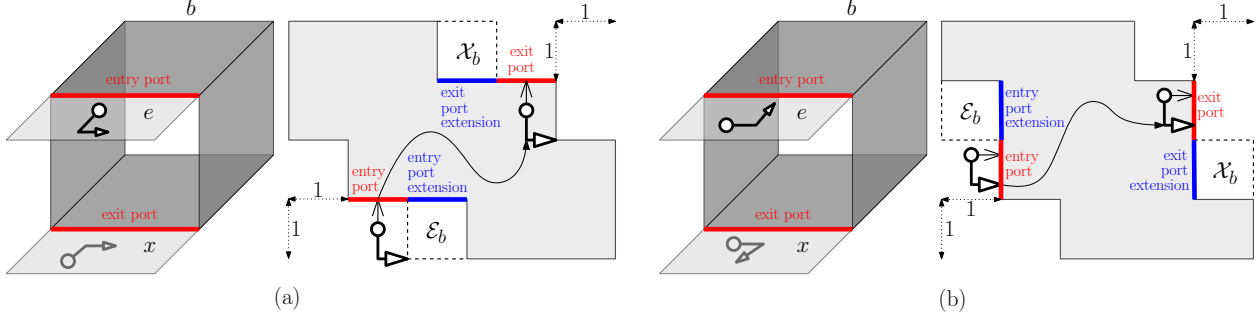


Figure 4: Inductive region for (a) HEAD-first unfolding (b) HAND-first unfolding.

before and after the combined (90° -rotation, reflection) transformation, because it extends in the direction of the HAND (HEAD) in a HEAD-first (HAND-first) unfolding. Similarly, the predecessor \leftarrow^x of d 's exit ring face is the same before and after the transformation. Thus the rules from Definition 1 for including \mathcal{E}_d and \mathcal{X}_d in the inductive region for d refer to the same ring faces before and after the transformation. These together show that, when applied to the unfolding net, this transformation turns a HEAD-first recursive unfolding of d into a HAND-first recursive unfolding of b . \square

Lemma 2 enables us to focus the rest of the paper on HEAD-first unfoldings only, with the understanding that the results transfer to HAND-first unfoldings.

4 Net Connections

We now discuss the type of connections that each HEAD-first unfolding net \mathcal{N}_b associated with a box b must provide to ensure that it connects to the rest of \mathcal{T} 's unfolding. To do so, we need a few more definitions.

Let e' (x') be the open ring face of \mathcal{T}_b that is adjacent to e (x) along the entry (exit) port. If $\stackrel{e}{\rightarrow}$ (\leftarrow^x) is open, let $\stackrel{e'}{\rightarrow}$ ($\leftarrow^{x'}$) be the open ring face adjacent to it along its side of unit length (see Figure 5). Note that, although e and $\stackrel{e}{\rightarrow}$ are ring faces from the same box by definition, ring faces e' and $\stackrel{e'}{\rightarrow}$ may be from different boxes (as in Figure 5b,c), and similarly for x' and $\leftarrow^{x'}$. Although these definitions may seem a bit intricate at this point, they will greatly simplify the description of our approach.

If b is not the root of \mathcal{T} , to ensure that b 's net connects to the rest of \mathcal{T} 's unfolding, it must provide type-1 or type-2 connection pieces placed along the boundary inside its inductive region. These connections are defined as follows:

- A *type-1 entry connection* consists of the ring face e' placed alongside the entry port. (See Figure 5(a,b) for examples.)
- A *type-1 exit connection* consists of the ring face x' placed alongside the exit port. (See Figure 5(b,c) for examples.)
- A *type-2 entry connection* is used when the ring face $\stackrel{e}{\rightarrow}$ is open and adjacent to \mathcal{T}_b , and consists of the ring face $\stackrel{e'}{\rightarrow}$ placed alongside the entry port extension. (See Figure 5c for an example.)
- A *type-2 exit connection* is used when the ring face \leftarrow^x is open and adjacent to \mathcal{T}_b , and consists of the ring face $\leftarrow^{x'}$ placed alongside the exit port extension. (See Figure 5a for an example.)

The unfolding of b begins (ends) on the type-1 or type-2 entry (exit) connection of b 's net. As we will show, the existence of these connections is enough to guarantee that b 's net connects to the rest of \mathcal{T} 's unfolding. In most cases, the connection to the rest of \mathcal{T} 's unfolding will be made along the port or port extension side of b 's type-1 or type-2 connection. In some cases though, the connection will be made along the left (right) side of b 's type-1 entry (exit) connection.

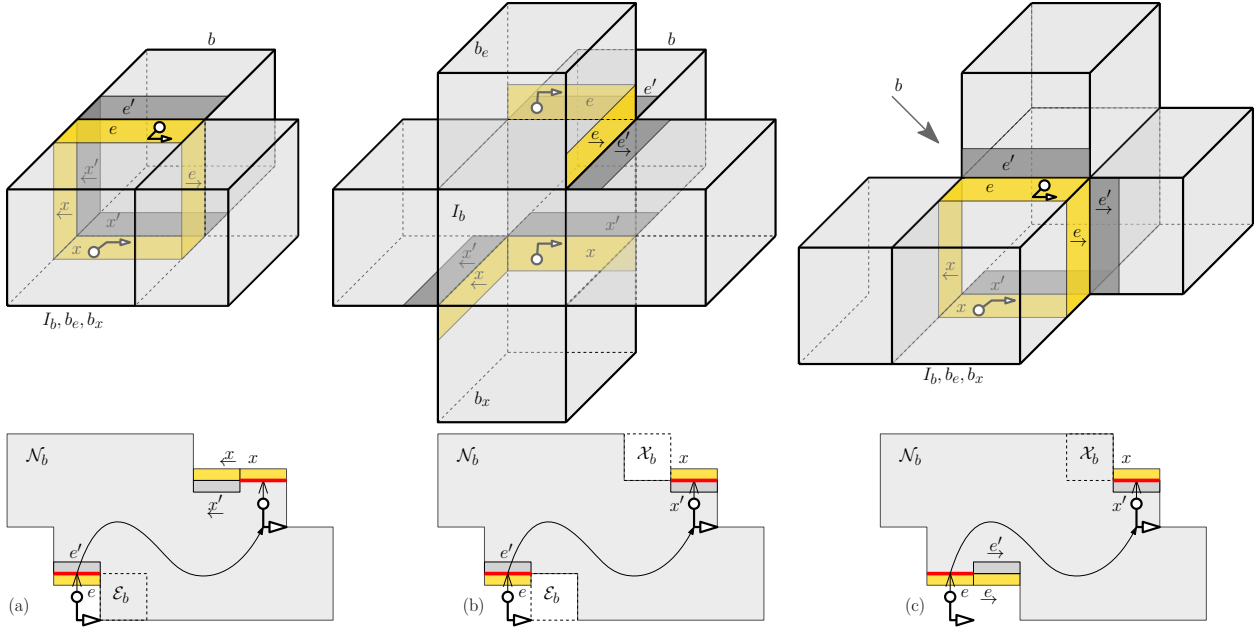


Figure 5: Net connections. (a) Type-1 entry connection, because \xrightarrow{e} is closed (so E_b is part of the inductive region); type-2 exit connection, because \xleftarrow{x} is open and adjacent to T_b (type-1 exit connection would also be allowed here) (b) Type-1 entry and exit connections, because \xrightarrow{e} and \xleftarrow{x} are non-adjacent to T_b ; they are both open, so E_b and X_b are not part of the inductive region (c) Type-2 entry connection, because \xrightarrow{e} is open and adjacent to T_b (type-1 entry connection would also be allowed here); type-1 exit connection, because \xleftarrow{x} is closed (so X_b is part of the inductive region). Note that the strips e, x, \xrightarrow{e} and \xleftarrow{x} highlighted along the nets do not necessarily attach to N_b ; they are included here for the purpose of illustrating the definitions.

5 Unfolding Invariants

We will make use of the following invariants tied to a recursive unfolding of a box $b \in \mathcal{T}$ other than the root box:

- (I1) The recursive unfolding of b produces an unfolding net N_b that fits within the inductive region and includes all open faces of T_b , with cuts restricted to a 4×4 refinement of the box faces.
- (I2) The unfolding net N_b provides the following entry and exit connections (see Figure 5):
 - (a) If \xrightarrow{e} is open and adjacent to a face in T_b , then N_b provides either a type-1 or type-2 entry connection. Otherwise, N_b provides a type-1 entry connection.
 - (b) If \xleftarrow{x} is open and adjacent to a face in T_b , then N_b provides either a type-1 or type-2 exit connection. Otherwise, N_b provides a type-1 exit connection.
- (I3) Open faces of b 's ring that are not used in N_b 's entry and exit connections can be removed from N_b without disconnecting N_b .

Invariant (I3) is sometimes employed in gluing two nets together, particularly in cases where the exit port of a box b does not align with the entry port of the box b' next visited by the unfolding path. In such cases, the unfolding algorithm may use ring pieces of b and b' identified by (I3) to form a bridge between their corresponding nets. Referring forward to Figure 12 for example, the strips R_N and T_E are removed from their respective nets N_N and N_E and used to connect the two nets. Similarly, the strips B_W and L_S are removed from N_W and N_S and used to connect N_W and N_S .

The following proposition follows immediately from the definition of the invariants (I1)-(I3) above.

Proposition 3. *If a net N_b satisfies invariants (I1)-(I3), then the net obtained after a 180° -rotation of N_b also satisfies invariants (I1)-(I3) (with entry and exit switching roles).*

Lemma 4. Let ξ be the unfolding path and \mathcal{N}_b the unfolding net produced by a recursive unfolding of b . Let $\overleftarrow{\xi}$ be the unfolding path traversed in reverse, starting at the exit port of \mathcal{N}_b and ending at the entry port of N , with the HEAD and HAND pointing in opposite direction. If \mathcal{N}_b satisfies the invariants (I1)-(I3), then the unfolding net induced by $\overleftarrow{\xi}$ also satisfies invariants (I1)-(I3).

Proof. The unfolding net $\widehat{\mathcal{N}}_b$ induced by $\overleftarrow{\xi}$ is a diagonal flip (180° -rotation) of \mathcal{N}_b . This along with Proposition 3 implies that $\widehat{\mathcal{N}}_b$ satisfies invariants (I1)-(I3). \square

6 Main Result

This section introduces our main result, which uses **Theorem 1** below. We note here that **Theorem 1** makes references to upcoming lemmas, which are organized into separate sections for clarity and ease of reference. So the main role of **Theorem 1** is to organize all unfolding cases into a structure that outlines the proof technique detailed in subsequent sections.

Theorem 1. Any box $A \in \mathcal{T}$ other than the root satisfies invariants (I1)-(I3) (listed in Section 5).

Proof. The proof is by strong induction on the height h of \mathcal{T}_A . The base case corresponds to $h = 0$ (i.e., A is a leaf).

Consider the unfolding of leaf box A depicted in Figure 2a: starting at A 's entry port, the unfolding path simply moves HEAD-first until it reaches A 's exit port. We now show that, when laid flat in the plane, the open faces of A form a net \mathcal{N}_A that satisfies invariants (I1)-(I3). First note that the net \mathcal{N}_A from Figure 2a fits within the inductive region and includes all open faces of A , therefore invariant (I1) is satisfied. To check (I2), observe that \mathcal{N}_A provides type-1 entry and exit connections, since $e' \in T_A$ and $x' \in B_A$ are positioned alongside the entry and exit ports. To check (I3), observe that the open ring faces of A not used in A 's entry or exit connections are the dark-shaded pieces from Figure 2a, and their removal does not disconnect \mathcal{N}_A . Thus \mathcal{N}_A also satisfies all three invariants.

The inductive hypothesis states that the theorem holds for any dual subtree of height h or less. To prove the inductive step, we consider a dual subtree \mathcal{T}_A of height $h + 1$, and prove that the theorem holds for the root A of \mathcal{T}_A .

First note that, because A is not the root of \mathcal{T} , A has a parent in \mathcal{T} . Also, since the height of \mathcal{T}_A is at least 1, A has at least one child in \mathcal{T}_A . By the inductive hypothesis, each child of A satisfies invariants (I1)-(I3). We discuss five cases, depending on the degree of A .

1. A is of degree 2: this case is settled by **Theorem 3**.
2. A is of degree 3: this case is settled by **Theorem 4**.
3. A is of degree 4: this case is settled by **Theorem 5**.
4. A is of degree 5: this case is settled by **Theorem 6**.
5. A is of degree 6: this case is settled by **Theorem 7**.

Having exhausted all cases, we conclude the result of this theorem. \square

Theorem 2. [Main result.] Any polycube tree \mathcal{O} can be unfolded into a net using a 4×4 refinement.

Proof. Let \mathcal{T} be the dual tree of \mathcal{O} and let $A \in \mathcal{T}$ be the root of \mathcal{T} (by definition, A is a node of degree one in \mathcal{T}). Assume without loss of generality that A has a back child J (if this is not the case, reorient \mathcal{O} to make this assumption hold). A recursive unfolding of A is depicted in Figure 6a: starting HEAD-first on the top face of A , the unfolding path recursively visits J and returns to the bottom face of A . The resulting net takes the shape depicted in Figure 6b.

By **Theorem 1**, J satisfies invariants (I1)-(I3), so its net \mathcal{N}_J takes the shape depicted in Figure 6b. Notice that $e_J \in T_A$ and $x_J \in B_A$. Since $\xrightarrow{e_J} \in R_A$ and $\xleftarrow{x_J} \in L_A$ are both open, the unit squares \mathcal{E}_J and \mathcal{X}_J (occupied in Figure 6b by R_A and L_A , respectively) do not belong to the inductive region for J . Furthermore, since $\xrightarrow{e_J}$ and $\xleftarrow{x_J}$ are adjacent to \mathcal{T}_J , invariant (I2) applied to J tells us that \mathcal{N}_J provides either type-1 or

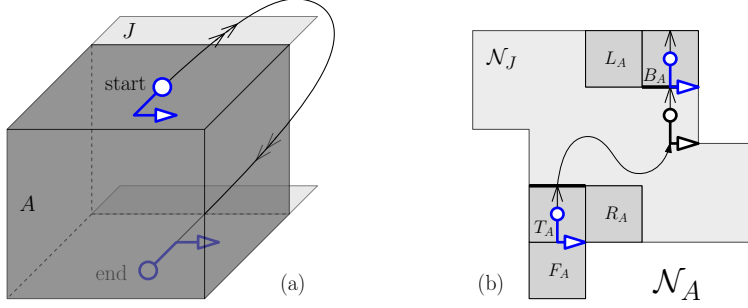


Figure 6: Unfolding of root A with back child J (a) unfolding path (b) unfolding net \mathcal{N}_A .

type-2 entry and exit connections. If of type-1, the entry (exit) connection attaches to T_A (B_A); otherwise, it attaches to R_A (L_A). In either case, the surface piece \mathcal{N}_A depicted in Figure 6b is connected. Invariant (I1) applied to J tells us that \mathcal{N}_J is a net that includes all open faces in the subtree \mathcal{T}_J rooted at J and uses a 4×4 refinement. This along with the fact that the open faces of A attach to \mathcal{N}_J without overlap settles this theorem. \square

The need for a 4×4 refinement will become clear later in Section 7.2, where we discuss a case that requires a 4-refinement along one dimension (depicted in Figure 10a).

7 Unfolding Algorithm

Our unfolding algorithm uses an unfolding path that begins on the top face of the root box of \mathcal{T} , recursively visits all nodes in the subtree rooted at the (unique) child of the root box, and ends on the bottom face of the root box (as depicted in Figure 6). The result is a net that includes all open faces of \mathcal{O} (as established by **Theorem 2**).

This section is dedicated to proving the five results referenced by **Theorem 1**. The unfolding algorithm is implicit in the proofs of these results. Here we provide a complete discussion for boxes of degrees 1, 2 and 6. For boxes of degree 3, 4, and 5, we select only a few representative cases that exemplify our main ideas. The reader can refer to the appendix for the remaining cases, which are very similar. (We do not include all cases here in order to avoid repetitiveness and improve the flow and clarity of our techniques.)

7.1 Unfolding Degree-2 Nodes

In this section we describe the recursive unfolding of a box $A \in \mathcal{T}$ of degree 2, and show that it satisfies the invariants (I1)-(I3) listed in Section 5.

Theorem 3. *Let $A \in \mathcal{T}$ be a degree-2 box. If A 's child satisfies invariants (I1)-(I3), then A satisfies invariants (I1)-(I3).*

Proof. Our analysis is split into four different cases, depending on the position of A 's child (note that A 's parent contributes one unit to A 's degree):

- Case 2.1 E is a child of A . This case is settled by Lemma 5.
- Case 2.2 W is a child of A . This case is settled by Lemma 6.
- Case 2.3 J is a child of A . This case is settled by Lemma 7.
- Case 2.4 N is a child of A . This case is settled by Lemma 8.

The case where S is a child of A is a vertical reflection of Case 2.4. \square

Lemma 5. *Let $A \in \mathcal{T}$ be a degree-2 node with parent I and child E (Case 2.1). If E satisfies invariants (I1)-(I3), then A satisfies invariants (I1)-(I3).*

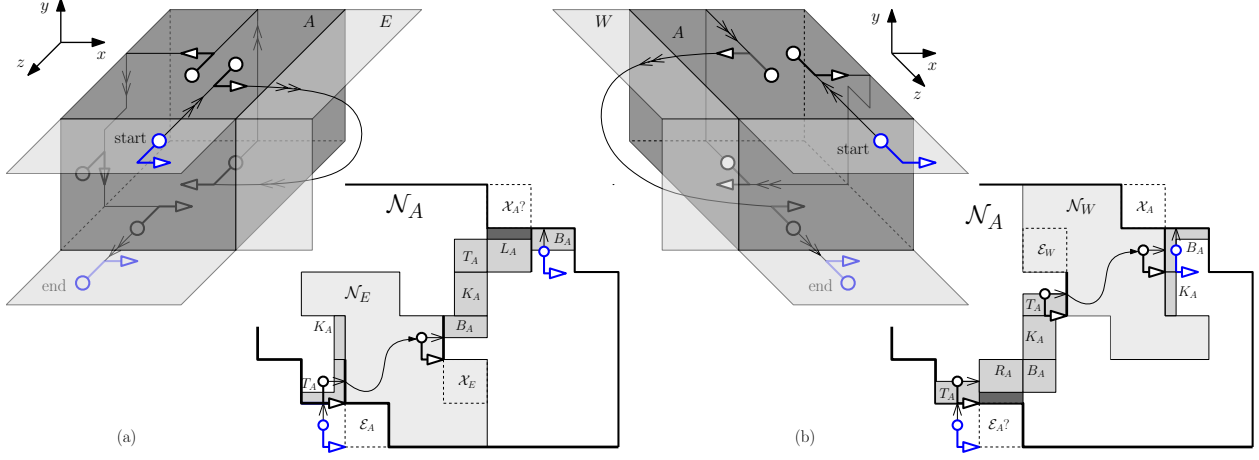


Figure 7: Unfolding of degree-2 box A with parent I and child (a) E (b) W .

Proof. Lemma 2 allows us to restrict our attention to HEAD-first unfoldings of A . The unfolding for this case is depicted in Figure 7a: starting at A 's entry port, the unfolding path moves HEAD-first to T_A , then proceeds HAND-first to recursively unfold E ; from E 's exit ring face on B_A , it proceeds HEAD-first up K_A to T_A ; from T_A , it proceeds HAND-first down L_A to B_A , and then moves HEAD-first on B_A to A 's exit port. We now show that, when visited in this order and laid flat in the plane, the open faces in \mathcal{T}_A form a net \mathcal{N}_A that satisfies invariants (I1)-(I3).

First note that the net \mathcal{N}_A in Figure 7a provides type-1 entry and exit connections, since $e'_A \in T_A$ and $x'_A \in B_A$ are positioned alongside its entry and exit ports. This shows that \mathcal{N}_A satisfies invariant (I2). Also note that (I3) is satisfied, because the only open ring face of A not used in \mathcal{N}_A 's entry or exit connections is the piece of L_A dark-shaded in Figure 7a (located below \mathcal{N}_A 's exit port extension), which can be removed from \mathcal{N}_A without disconnecting \mathcal{N}_A .

It remains to show that \mathcal{N}_A satisfies invariant (I1). We begin with the following set of observations showing that the net \mathcal{N}_E produced by the recursive unfolding of E connects to the pieces of T_A , K_A , and B_A placed alongside its boundary:

- Observe first that the entry (exit) port in the recursive unfolding of E is the top (bottom) edge of R_A . With this entry (exit) port, E 's entry (exit) ring face e_E (x_E) is on T_A (B_A) and its successor (predecessor) $\xrightarrow{e_E}$ ($\xleftarrow{x_E}$) is on K_A (F_A).
- Since $\xrightarrow{e_E} \in K_A$ is open, the unit square \mathcal{E}_E (occupied by $\xrightarrow{e_E}$ in Figure 7a) is not part of the inductive region for E . Since $\xrightarrow{e_E}$ is also adjacent to \mathcal{T}_E , invariant (I2) applied to E tells us that \mathcal{N}_E provides either a type-1 or type-2 entry connection. If \mathcal{N}_E provides a type-1 entry connection, then e'_E is located alongside its entry port, and it connects (by definition) to $e_E \in T_A$ located on the other side of its entry port (see Figure 7a); if \mathcal{N}_E provides a type-2 connection, then $\xrightarrow{e'_E}$ is located alongside its entry port extension, and it connects (by definition) to $\xrightarrow{e_E} \in K_A$ located on the other side of its entry port extension.
- Since $\xleftarrow{x_E} \in F_A$ is closed, \mathcal{X}_E is part of E 's inductive region and the invariant (I2) applied to E tells us that \mathcal{N}_E provides a type-1 exit connection. This means that x'_E is located alongside \mathcal{N}_E 's exit port, and it connects (by definition) to the piece of $x_E \in B_A$ located on the other side of its exit port (see Figure 7a).

Because invariant (I1) tells us that \mathcal{N}_E is connected and because the pieces of A placed alongside \mathcal{N}_E connect to \mathcal{N}_E 's entry and exit connections, we can conclude that \mathcal{N}_A is connected. By invariant (I1) applied to E , the net \mathcal{N}_E includes all open faces in \mathcal{T}_E using a 4×4 refinement. This along with the fact that \mathcal{N}_A includes T_A , L_A , B_A , and K_A (which are A 's open faces) using a 4×4 refinement shows that \mathcal{N}_A includes all open faces of \mathcal{T}_A using a 4×4 refinement. Finally, \mathcal{N}_A fits within A 's inductive region as illustrated in

Figure 7a, noting that no part of \mathcal{N}_A lies within the cells marked \mathcal{E}_A and \mathcal{X}_A (which renders a discussion of whether or not these cells are part of its inductive region unnecessary). Thus we can conclude that \mathcal{N}_A satisfies invariant (I1). \square

Lemma 6. *Let $A \in \mathcal{T}$ be a degree-2 node with parent I and child W (Case 2.2). If W satisfies invariants (I1)-(I3), then A satisfies invariants (I1)-(I3).*

Proof. The unfolding for this case is depicted in Figure 7b. Note that this unfolding path can be obtained by rotating the path from Figure 7a by 180° . This along with Lemmas 4 and 5 implies that the net \mathcal{N}_A from Figure 7b satisfies invariants (I1)-(I3). \square

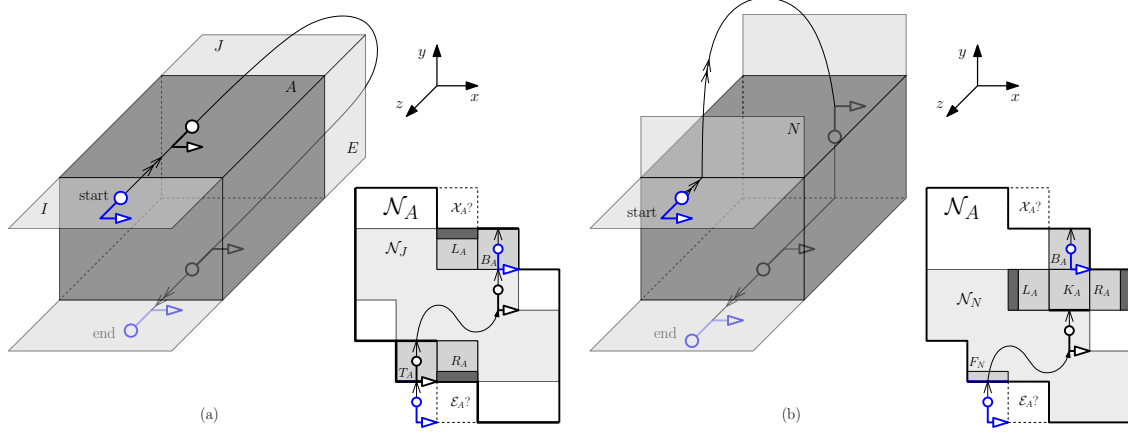


Figure 8: Unfolding of degree-2 box A with parent I and child (a) J (b) N .

Lemma 7. *Let $A \in \mathcal{T}$ be a degree-2 node with parent I and child J (Case 2.3). If J satisfies invariants (I1)-(I3), then A satisfies invariants (I1)-(I3).*

Proof. Consider the unfolding depicted in Figure 8a, and notice its similarity with the unfolding of the root box from Figure 6. We show that the unfolding \mathcal{N}_A from Figure 8a satisfies invariants (I1)-(I3).

Note that \mathcal{N}_A provides a type-1 entry connection ($e'_A \in T_A$) and a type-1 exit connection ($x'_A \in B_A$), and therefore it satisfies invariant (I2). Since $\xrightarrow{e_J} \in R_A$ ($\xleftarrow{x_J} \in L_A$) is open, \mathcal{E}_J (\mathcal{X}_J) is not part of J 's inductive region. Furthermore, since $\xrightarrow{e_J}$ ($\xleftarrow{x_J}$) is adjacent to \mathcal{T}_J , invariant (I2) applied to J tells us that \mathcal{N}_J provides a type-1 or type-2 entry (exit) connection, which attaches to T_A or R_A (B_A or L_A). Thus the net \mathcal{N}_A is connected.

By invariant (I1), \mathcal{N}_J covers all open faces in \mathcal{T}_J using a 4×4 refinement. Since \mathcal{N}_A includes the open faces of A without any refinement, we conclude that \mathcal{N}_A includes all open faces of \mathcal{T}_A . Noting that \mathcal{N}_A fits within A 's inductive region (and doesn't use the cells marked \mathcal{E}_A and \mathcal{X}_A), we conclude that \mathcal{N}_A satisfies invariant (I1). Finally, the open ring faces of A not used in its entry and exit connections (dark-shaded in Figure 8a) can be removed from \mathcal{N}_A without disconnecting \mathcal{N}_A , therefore \mathcal{N}_A satisfies invariant (I3). \square

Lemma 8. *Let $A \in \mathcal{T}$ be a degree-2 node with parent I and child N (Case 2.4). If N satisfies invariants (I1)-(I3), then A satisfies invariants (I1)-(I3).*

Proof. Consider the unfolding depicted in Figure 8b. Note that $\xrightarrow{e_A} = \xrightarrow{e_N} \in R_I$ is not adjacent to \mathcal{T}_N , therefore \mathcal{N}_N will provide a type-1 entry connection (by (I2) applied to N), which is also a type-1 entry connection for A (because $e'_N = e'_A \in F_N$). Note that \mathcal{N}_A also provides a type-1 exit connection $x'_A \in B_A$, therefore \mathcal{N}_A satisfies invariant (I2). Since $\xleftarrow{x_N} \in L_A$ is open, the unit square \mathcal{X}_N (occupied by L_A in Figure 8b) does not belong to the inductive region for N . Furthermore, since $\xleftarrow{x_N}$ is adjacent to \mathcal{T}_N , invariant (I2) applied to N tells us that \mathcal{N}_N provides a type-1 or type-2 exit connection, which attaches to K_A or L_A (located along the exit port and exit port extension). Thus the net \mathcal{N}_A is connected. Arguments similar to those in Lemma 7 complete the proof that \mathcal{N}_A satisfies (I1) and show that it satisfies invariant (I3). \square

7.2 Unfolding Degree-3 Nodes

In this section we describe the recursive unfolding of a box $A \in \mathcal{T}$ of degree 3, and show that it satisfies the invariants (I1)-(I3) listed in Section 5.

Theorem 4. *Let $A \in \mathcal{T}$ be a degree-3 box. If A 's children satisfy invariants (I1)-(I3), then A satisfies invariants (I1)-(I3).*

Proof. Our analysis is split into five different cases, depending on the position of A 's children:

Case 3.1 E and J are children of A . The case where W and J are children of A is a horizontal reflection of this case, with the unfolding path traversed in reverse.

Case 3.2 N and J are children of A . The case where S and J are children of A is a vertical reflection of this case, with the unfolding path traversed in the reverse.

Case 3.3 E and W are children of A .

Case 3.4 N and S are children of A .

Case 3.5 N and E are children of A . This is the same as the case where S and W are children of A , rotated by 180° about the z -axis (so the unfolding path is the same, but traversed in reverse).

Case 3.6 N and W are children of A . This is the same as the case where S and E are children of A , rotated by 180° about the z -axis (so the unfolding path is the same, but traversed in reverse).

The rest of this section is devoted to a detailed analysis of Cases 3.1 and 3.2. Case 3.2 in particular is special because it requires 4×4 refinement. Cases 3.3 through 3.5, while employing different unfolding paths, use similar arguments in their correctness proofs and are detailed in Appendix A. Note that the ability to "traverse in reverse" in some of the cases listed above follows from Lemma 4. \square

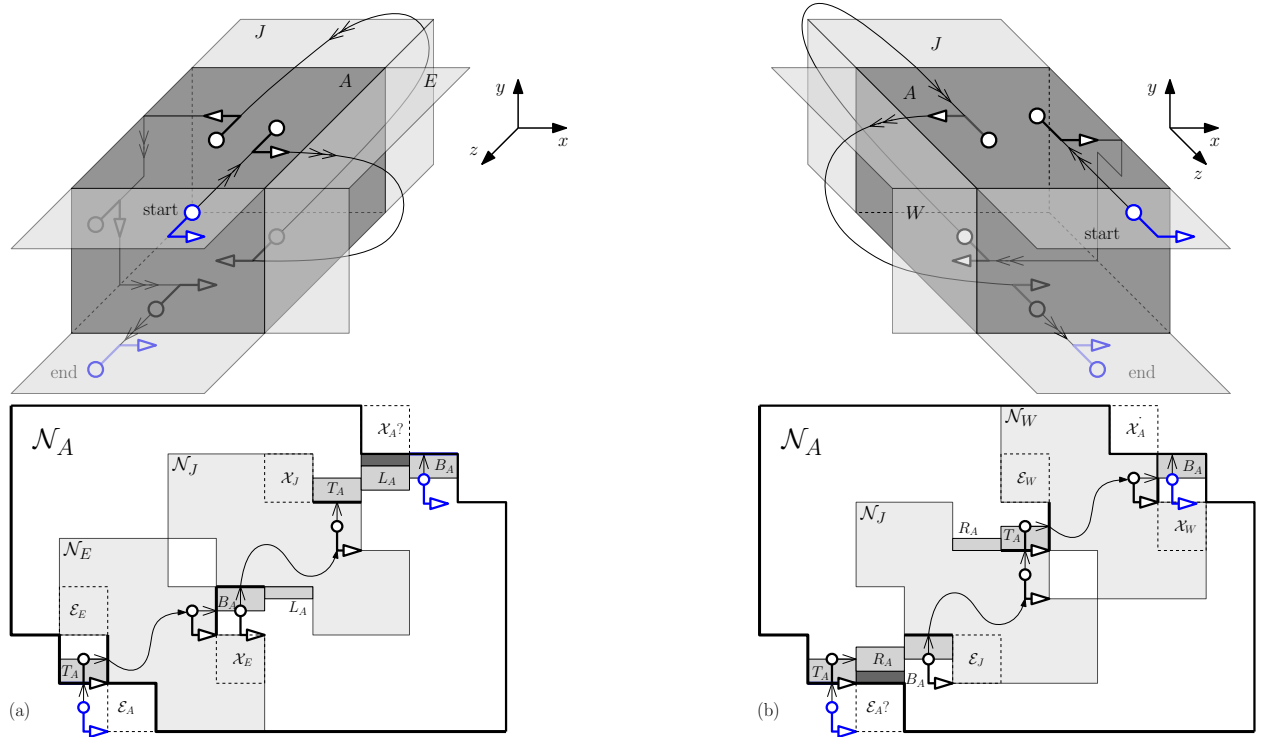


Figure 9: Unfolding of degree-3 box A with children J and (a) E (b) W .

Lemma 9. *Let $A \in \mathcal{T}$ be a degree-3 node with parent I and children E and J (Case 3.1). If A 's children satisfy invariants (I1)-(I3), then A satisfies invariants (I1)-(I3).*

Proof. The unfolding for this case is depicted in Figure 9a. Observe that it is a generalization of the degree-2 unfolding from Figure 7a, where the unfolded face K_A is replaced by the recursive unfolding of child J . Since the two unfoldings and the proofs of their correctness are very similar, we only point out the differences here:

- Because the ring face $\xrightarrow{e_E} \in K_A$ is closed, \mathcal{E}_E is part of E 's inductive region. By invariant (I2) applied to E , \mathcal{N}_E provides a type-1 entry connection, which connects to $e_E \in T_A$.
- Observe that the entry (exit) port for J is the bottom (top) edge of F_J and so the entry (exit) ring face $e_J (x_J)$ is part of $B_A (T_A)$. Because $\xrightarrow{e_J} \in L_A$ is open, the unit square \mathcal{E}_J (occupied by $\xrightarrow{e_J}$ in Figure 9a) is not part of J 's inductive region. Furthermore, since $\xrightarrow{e_J}$ is adjacent to \mathcal{T}_J , invariant (I2) applied to J tells us that \mathcal{N}_J provides a type-1 or type-2 entry connection: if type-1, then it connects to the piece $e_J \in B_A$; if type-2, then it connects to $\xrightarrow{e_J} \in L_A$.
- Because the ring face $\xleftarrow{x_J} \in R_A$ is closed, \mathcal{X}_J is part of E 's inductive region. By invariant (I2) applied to J , \mathcal{N}_J provides a type-1 exit connection, which connects to $x_J \in T_A$.

These differences combined with arguments similar to those in Lemma 5 show that \mathcal{N}_A satisfies invariants (I1)-(I3). \square

The case where W and J are children of A shown in Figure 9b is the reverse of the case shown in Figure 9a. This along with Lemma 4 implies that the net \mathcal{N}_A from Figure 9b also satisfies invariants (I1)-(I3).

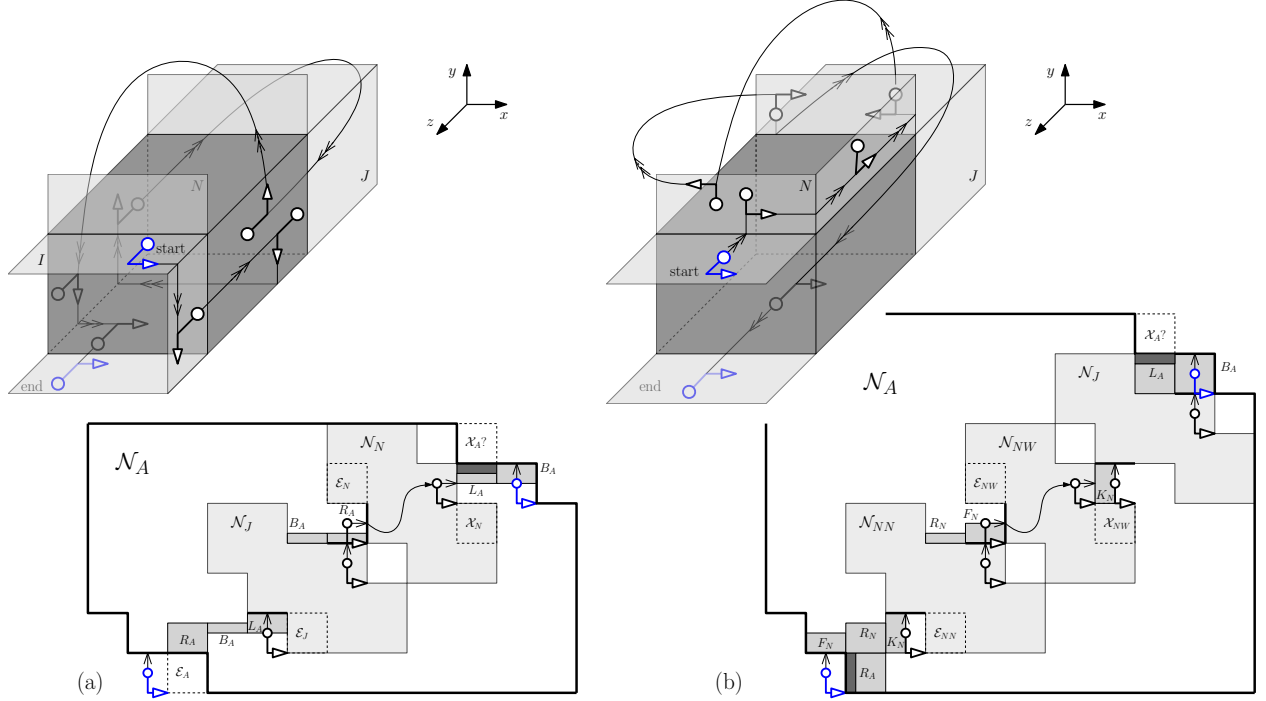


Figure 10: Unfolding of degree-3 box A with parent I and children N and J (a) R_I open. Note that A requires a 4-refinement along the z -dimension to be able to generate the strips of B_A and L_A shown here.

(b) R_I closed (so R_N open).

Lemma 10. Let $A \in \mathcal{T}$ be a degree-3 node with parent I and children N and J (Case 3.2). If A 's children satisfy invariants (I1)-(I3), then A satisfies invariants (I1)-(I3).

Proof. We discuss two situations, depending on whether R_I is open or closed. Assume first that R_I is open, and consider the unfolding depicted in Figure 10a. Note that $\xrightarrow{e_A} \in R_I$ is open and adjacent to \mathcal{T}_A , and \mathcal{N}_A provides a type-2 entry connection $\xrightarrow{e'_A} \in R_A$. Also note that \mathcal{N}_A provides a type-1 exit connection $x'_A \in B_A$.

These together show that \mathcal{N}_A satisfies invariant (I2). The following observations support our claim that \mathcal{N}_A satisfies invariant (I1):

- The entry and exit ring faces for J are $e_J \in L_A$ and $x_J \in R_A$. Since $\xrightarrow{e_J} \in T_A$ is closed, \mathcal{N}_J provides a type-1 entry connection, which attaches to $e_J \in L_A$. Since $\xleftarrow{x_J} \in B_A$ is open and adjacent to \mathcal{T}_J , the unit square \mathcal{X}_J (occupied by $\xleftarrow{x_J}$ in Figure 10a) does not belong to the inductive region for J , and \mathcal{N}_J may provide a type-1 or type-2 exit connection: if type-1, it attaches to the ring face $x_J \in R_A$ placed alongside its exit port; if type-2, it connects to the ring face $\xrightarrow{x_J} \in B_A$ placed alongside its exit port extension.
- The entry and exit ring faces for N are $e_N \in R_A$ and $x_N \in L_A$. Note that \mathcal{N}_N provides type-1 entry and exit connections (since $\xrightarrow{e_N} \in F_A$ and $\xleftarrow{x_N} \in K_A$ are both closed), which attach to the pieces of the entry and exit ring faces placed alongside its entry and exit ports.

Finally, note that the only open ring face of A not involved in A 's entry and exit connections is the dark-shaded piece of L_A from Figure 10a, whose removal does not disconnect \mathcal{N}_A . Thus \mathcal{N}_A satisfied (I3) as well.

Assume now that R_I is closed, and consider the unfolding depicted in Figure 10b. Note that \mathcal{N}_A provides type-1 entry and exit connections $e'_A \in F_N$ and $x'_A \in B_N$, therefore it satisfies invariant (I2). The following observations support our claim that \mathcal{N}_A satisfies invariant (I1):

- The entry and exit ring faces for NN , NW and J are as follows: $e_{NN} \in K_N$ and $x_{NN} \in F_N$; $e_{NW} \in F_N$ and $x_{NW} \in K_N$; and $e_J \in K_N$ and $x_J \in B_A$.
- \mathcal{N}_{NN} , \mathcal{N}_{NW} and \mathcal{N}_J provide type-1 entry connections. This is because $\xrightarrow{e_{NN}} \in L_N$ is closed, $\xrightarrow{e_{NW}} \in B_N$ is closed, and $\xrightarrow{e_J} \in R_N$ is not adjacent to \mathcal{T}_J .
- Since $\xleftarrow{x_{NN}} \in R_N$ is open, the unit square \mathcal{X}_{NN} (occupied by $\xleftarrow{x_{NN}}$ in Figure 10b) does not belong to the inductive region for NN . Similarly, since $\xleftarrow{x_J} \in L_A$ is open, the unit square \mathcal{X}_J (occupied by L_A in Figure 10b) does not belong to the inductive region for J .
- Since $\xleftarrow{x_{NW}} \in T_N$ is closed, \mathcal{N}_{NW} provides a type-1 exit connection.
- Since $\xrightarrow{e_A} \in R_I$ is closed, the unit square \mathcal{E}_A (occupied by R_A in Figure 10b) belongs to the inductive region for A .

Finally, note that the removal of the open ring faces of A not involved in A 's entry and exit connections (shown dark-shaded in Figure 10b) does not disconnect \mathcal{N}_A . Thus \mathcal{N}_A satisfies (I3) as well. \square

As a side note, the unfolding from Figure 10a is the first unfolding example that requires a 4-refinement along one dimension of the grid: one $1/4 \times 1$ strip of B_A is needed to transition from R_A to L_A ; one $1/4 \times 1$ strip of B_A is needed alongside \mathcal{N}_J 's exit port extension, to connect to the type-2 connection that \mathcal{N}_J may provide; and one $1/2 \times 1$ strip of B_A is needed alongside \mathcal{N}_A 's exit port, so that it remains connected to the piece of L_A to its left, once the dark-shaded ring face that lies on L_A has been removed.

7.3 Unfolding Degree-4 Nodes

In this section we describe the recursive unfolding of a box $A \in \mathcal{T}$ of degree 4, and show that it the invariants (I1)-(I3) listed in Section 5.

Theorem 5. *Let $A \in \mathcal{T}$ be a degree-4 box. If A 's children satisfy invariants (I1)-(I3), then A satisfies invariants (I1)-(I3).*

Proof. Our analysis is split into seven different cases, depending on the position of A 's children:

Case 4.1 J , E and W are children of A .

Case 4.2 N , E and W are children of A . The case where S , E and W are children of A is a vertical reflection of this case.

Case 4.3 N, E and J are children of A . The case where S, W and J are children of A is a 180° -rotation about the z -axis of this case.

Case 4.4 N, W and J are children of A . The case where S, E and J are children of A is a 180° -rotation about the z -axis of this case.

Case 4.5 N, E and S are children of A .

Case 4.6 N, W and S are children of A .

Case 4.7 N, J and S are children of A .

It can be verified that this is an exhaustive list of all possible cases for a degree-4 node. Case 4.1 is settled by Lemma 11. Cases 4.2 through 4.7, while employing different unfolding paths, use similar arguments in their correctness proofs and are detailed in Appendix B. \square

Lemma 11. *Let $A \in \mathcal{T}$ be a degree-4 node with parent I and children J, E and W (Case 4.1). If A 's children satisfy invariants (I1)-(I3), then A satisfies invariants (I1)-(I3).*

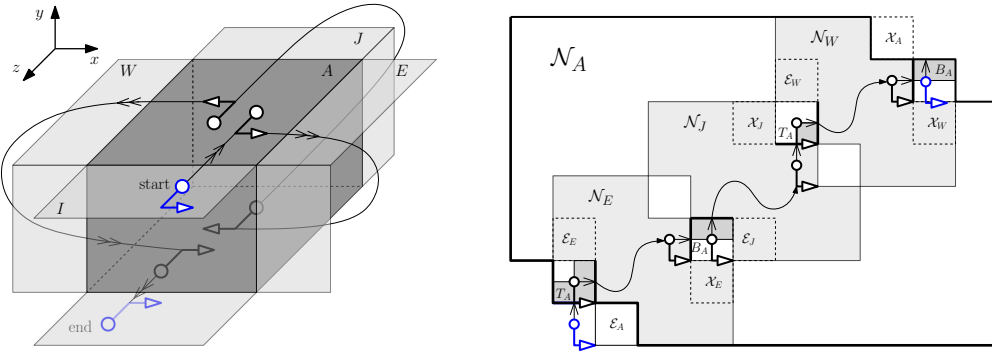


Figure 11: Unfolding of degree-4 box A with children J, E and W .

Proof. Consider the unfolding depicted in Figure 11, and note that it is a generalization of the degree-3 unfolding from Figure 9a, where the unfolded face L_A is replaced by the recursive unfolding of child W . Since the two unfoldings and their proofs are very similar, we only point out the differences here:

- Because $\xrightarrow{e_J} \in L_A$ is closed, \mathcal{E}_J is part of J 's inductive region and \mathcal{N}_J provides a type-1 entry connection which connects to $e_J \in B_A$.
- Observe that the entry (exit) port for W is the top (bottom) edge of R_W and so the entry (exit) ring face e_W (x_W) is part of T_A (B_A). Because $\xrightarrow{e_W} \in F_A$ ($\xleftarrow{x_W} \in K_A$) is closed, \mathcal{E}_W (\mathcal{X}_W) is part of W 's inductive region, and \mathcal{N}_W provides a type-1 entry (exit) connection which connects to the piece of $e_W \in T_A$ ($x_W \in B_A$) placed along \mathcal{N}_W 's entry (exit) port.

These differences combined with arguments similar to those in Lemma 9 show that \mathcal{N}_A satisfies invariants (I1) and (I2). Finally note that (I3) is trivially satisfied, because all of A 's open ring faces are used in its entry and exit connections. We therefore conclude that \mathcal{N}_A from Figure 11 satisfies invariants (I1)-(I3). \square

7.4 Unfolding Degree-5 Nodes

In this section we describe the recursive unfolding of a box $A \in \mathcal{T}$ of degree 5, and show that it satisfies the invariants (I1)-(I3) listed in Section 5.

Theorem 6. *Let $A \in \mathcal{T}$ be a degree-5 box. If A 's children satisfy invariants (I1)-(I3), then A satisfies invariants (I1)-(I3).*

Proof. Our analysis is split into four different cases, depending on the position of A 's children:

Case 5.1 J is not a child of A (so N, E, W and S are children of A).

Case 5.2 W is not a child of A (so N, E, J and S are children of A).

Case 5.3 E is not a child of A (so N, W, J and S are children of A).

Case 5.4 N is not a child of A (so E, W, J and S are children of A). The case when S is not a child of A is a vertical reflection of this case.

It can be verified that this is an exhaustive list of all possible cases for a degree-5 node. Case 5.1 is settled by Lemma 13. Cases 5.2 through 5.4, while employing different unfolding paths, use similar arguments in their correctness proofs and are detailed in Appendix C. \square

Before getting into details on Case 5.1, we introduce a preliminary lemma that will simplify our analysis.

Lemma 12. *Let $A \in \mathcal{T}$ be a degree-5 node with parent I and children N, E, W and S . Then either N and S are both non-junction boxes, or else E and W are both non-junction boxes.*

Proof. Assume to the contrary that at least one box in each pair (N, S) and (E, W) – say, N and E – is a junction (the argument for any choice of junctions is the same). This implies that N has a back neighbor (because any other neighbor position that would render N a junction would also render a loop in \mathcal{T}), and similarly for E . Note however that NJ and EJ meet at an edge, therefore NJ must have either a south or an east neighbor (because \mathcal{O} is homeomorphic to a sphere). However, each of these cases renders a cycle in \mathcal{T} , a contradiction. \square

Lemma 13. *Let $A \in \mathcal{T}$ be a degree-5 node with parent I and children N, E, W and S (Case 5.1). If A 's children satisfy invariants (I1)-(I3), then A satisfies invariants (I1)-(I3).*

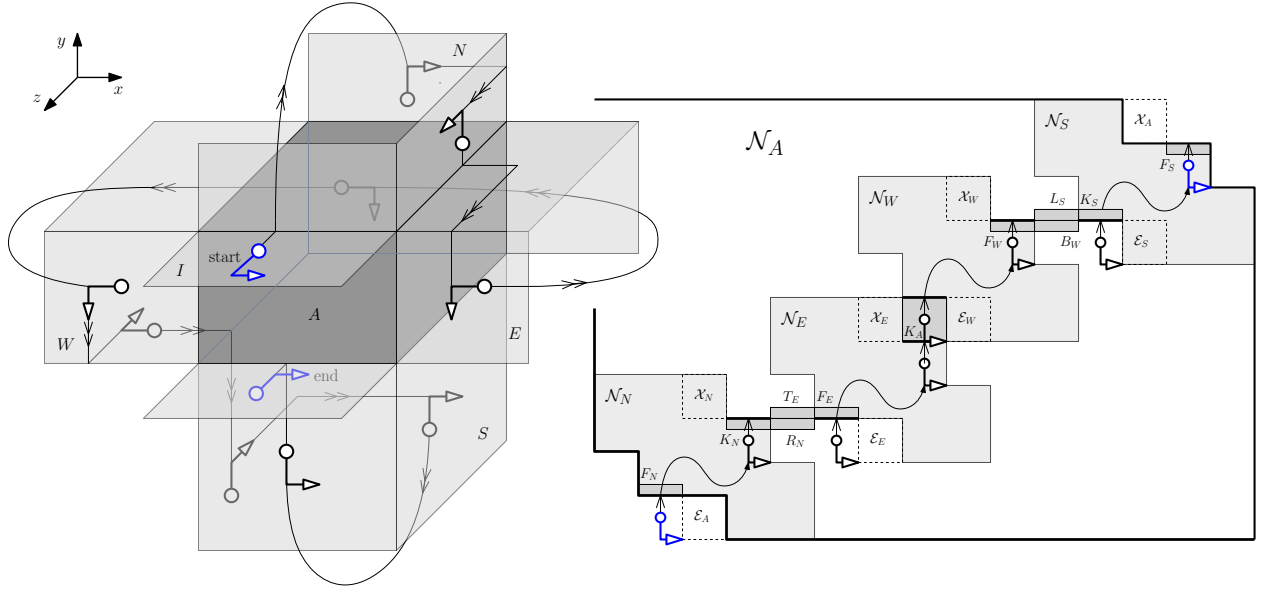


Figure 12: Unfolding of degree-5 box A with children N, E, W and S (N and S are non-junctions).

Proof. By Lemma 12, either N and S are both non-junctions, or E and W are both non-junctions. Assume first that N and S are both non-junctions and consider the unfolding depicted in Figure 12: starting at A 's entry port, the unfolding path proceeds HEAD-first to recursively unfold N ; upon reaching N 's exit port on K_N , it moves HAND-first to R_N , HEAD-first to T_E , HAND-first to F_E , then proceeds HEAD-first to recursively unfold E and W ; upon reaching W 's exit port on F_W , it moves HAND-first to S_W , HEAD-first to L_S , HAND-first to K_S , then proceeds HEAD-first to recursively unfold S , ending at A 's exit port. (Note that both K_N and K_S are open, since N and S are non-junctions.) We now show that, when visited in this order and laid flat in the plane, the open faces in \mathcal{T}_A form a net \mathcal{N}_A that satisfies invariants (I1)-(I3).

We start by showing that \mathcal{N}_A that satisfies invariant (I2). Note that $\xrightarrow{e_A} = \xrightarrow{e_N} \in R_I$ is open but not adjacent to \mathcal{T}_N , therefore \mathcal{N}_N will provide a type-1 entry connection (by (I2) applied to N), which is also a

type-1 entry connection for A (because $e'_N = e'_A \in F_N$). Similarly, $\xleftarrow{x_A} = \xleftarrow{x_S} \in L_I$ is open but not adjacent to \mathcal{T}_S , therefore S will provide a type-1 exit connection (by (I2) applied to S), which is also a type-1 exit connection for A (because $x'_S = x'_A \in F_S$). This shows that \mathcal{N}_A satisfies invariant (I2). Also note that (I3) is trivially satisfied, because A has no open ring faces.

It remains to show that \mathcal{N}_A satisfies invariant (I1). We begin by showing that \mathcal{N}_A is connected:

- Observe that the exit port for N is the top edge of K_A , and so N 's exit ring face x_N is on K_A . Its successor $\xrightarrow{x_N}$ is therefore on L_A and is closed. Invariant (I2) applied to N tells us that \mathcal{N}_N provides a type-1 exit connection $x'_N \in K_N$ alongside its exit port.
- When the unfolding path reaches N 's exit port, it deviates from prior unfoldings in that it doesn't move onto $x_N \in K_A$. Instead it stays on N and moves HAND-first across K_N to R_N (which is open because, if there were a box NE adjacent to it, then boxes NE, E, A, N would form a cycle). Therefore, a new technique described here is used to connect \mathcal{N}_N to the rest of \mathcal{N}_A . Note that the ring face of N located along the bottom of R_N is adjacent to $x'_N \in K_N$. In addition, this ring face is not used as an entry or exit connection in \mathcal{N}_N (because \mathcal{N}_N has type-1 entry/exit connections), so by invariant (I3) applied to N , it can be relocated outside of \mathcal{N}_N without disconnecting \mathcal{N}_N . We relocate it to the right of \mathcal{N}_N 's exit port, where it connects to \mathcal{N}_N 's type-1 exit connection $x'_N \in K_N$, as shown in Figure 12. This relocated piece of R_N serves as a bridge to the unfolding of the next box E .
- Next we turn to \mathcal{N}_E . The recursive unfolding applied to E uses the front edge of R_A for its entry port and the back edge of R_A for its exit port. With this unfolding, $e'_E \in F_E$, $e_E \in R_I$, and while $\xrightarrow{e_E} \in B_I$ is open, it is not adjacent to \mathcal{T}_E . Therefore the invariant (I2) applied to E tells us that it provides a type-1 entry connection. Similarly, $x_E \in K_A$ and $\xleftarrow{x_E} \in T_A$ is closed. Thus \mathcal{N}_E also provides a type-1 exit connection. The ring face of E located along the left edge of T_E is not used as an entry or exit connection for E and so by invariant (I3) (applied to E), it can be relocated outside of \mathcal{N}_E without disconnecting it. In the unfolding in Figure 12, it is relocated to the left of \mathcal{N}_E 's entry port. This relocated piece of T_E serves as a bridge to the unfolding of the previous box N . Thus the two relocated ring faces (one a piece of R_N taken from \mathcal{N}_N and the other a piece of T_E taken from \mathcal{N}_E) form a bridge between the exit connection $x'_N \in K_N$ of \mathcal{N}_N and the entry connection $e'_E \in F_E$ of \mathcal{N}_E . Finally, \mathcal{N}_E 's type-1 exit connection x'_E connects to $x_E \in K_A$ shown unfolded alongside \mathcal{N}_E 's exit port.
- Similar arguments hold for \mathcal{N}_W . Note that the entry (exit) port for W is the back (front) edge of L_A . Also note that $\xrightarrow{e_W} \in B_A$ is closed and $\xleftarrow{x_W} \in T_I$ is open but not adjacent to \mathcal{T}_W , therefore \mathcal{N}_W provides type-1 entry and exit connections. Its entry connection attaches to $e_W \in K_A$ and its exit connection attaches to the ring face of W located along the right edge of B_W , which has been relocated right of the exit port of \mathcal{N}_W .
- Similar arguments hold for \mathcal{N}_S . Note that the entry (exit) port for S is the back (front) edge of B_A . Also note that $\xrightarrow{e_S} \in R_A$ is closed, therefore \mathcal{N}_S provides a type-1 entry connection $e'_S \in K_S$. Its entry connection attaches to the ring face of S located along the top edge of L_S , which has been relocated left of the entry port of \mathcal{N}_S .

We conclude that \mathcal{N}_A is connected. By invariant (I1), $\mathcal{N}_N, \mathcal{N}_E, \mathcal{N}_W$ and \mathcal{N}_S include all open faces in $\mathcal{T}_N, \mathcal{T}_E, \mathcal{T}_W$ and \mathcal{T}_S respectively, using a 4×4 refinement. Observe that the net \mathcal{N}_A from Figure 12 also includes the open face K_A of A without any refinement. This shows that \mathcal{N}_A includes all open faces in \mathcal{T}_A using a 4×4 refinement. Finally, \mathcal{N}_A fits within A 's inductive region (as illustrated in Figure 12), noting that it does not utilize \mathcal{E}_A or \mathcal{X}_A . We therefore conclude that \mathcal{N}_A satisfies invariant (I1).

The case where E are W are non-junctions can be reduced to the case where N are S are non-junctions using the method depicted in Figure 13: from the entry port, the unfolding proceeds HAND-first to R_I (note that I is a non-junction in our context, so both T_I and R_I are open), then follows the path from Figure 12 (imagine the box from Figure 12 rotated clockwise by 90° , so that its entry guide aligns with the guide on R_I from Figure 13). Then the net labeled \mathcal{N}'_A in Figure 13 is identical to the net from Figure 12. From the exit port of \mathcal{N}'_A on L_I , the unfolding proceeds HAND-first to the exit port of \mathcal{N}_A on B_I .

We have already established that \mathcal{N}'_A satisfies invariants (I1)-(I3). Now note that the net \mathcal{N}'_A from Figure 12 provides type-1 entry and exit connections, which implies that the net \mathcal{N}_A from Figure 13 provides

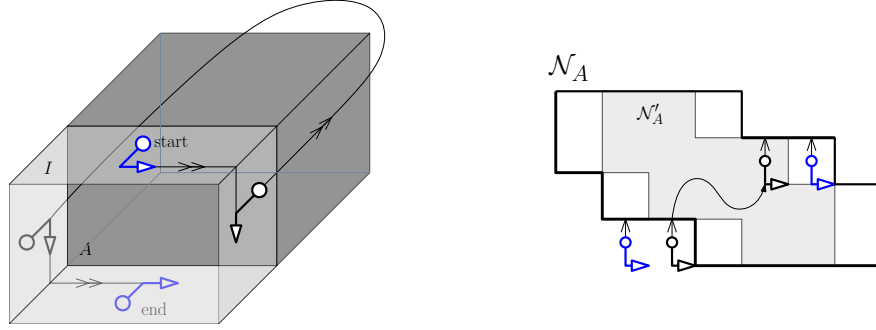


Figure 13: Unfolding of box A with non-junction parent I .

type-2 entry and exit connections. These together with the fact that $\xrightarrow{e_A} \in R_I$ and $\xleftarrow{x_A} \in L_I$ are open and adjacent to \mathcal{T}_A , imply that \mathcal{N}_A satisfies invariants (I1)-(I3). \square

7.5 Unfolding Degree-6 Nodes

The following observation follows immediately from the tree structure of \mathcal{T} .

Proposition 14. *Every neighbor of a degree-6 node in \mathcal{T} is a connector or a leaf.*

We now show that invariants (I1)-(I3) hold for any degree-6 box.

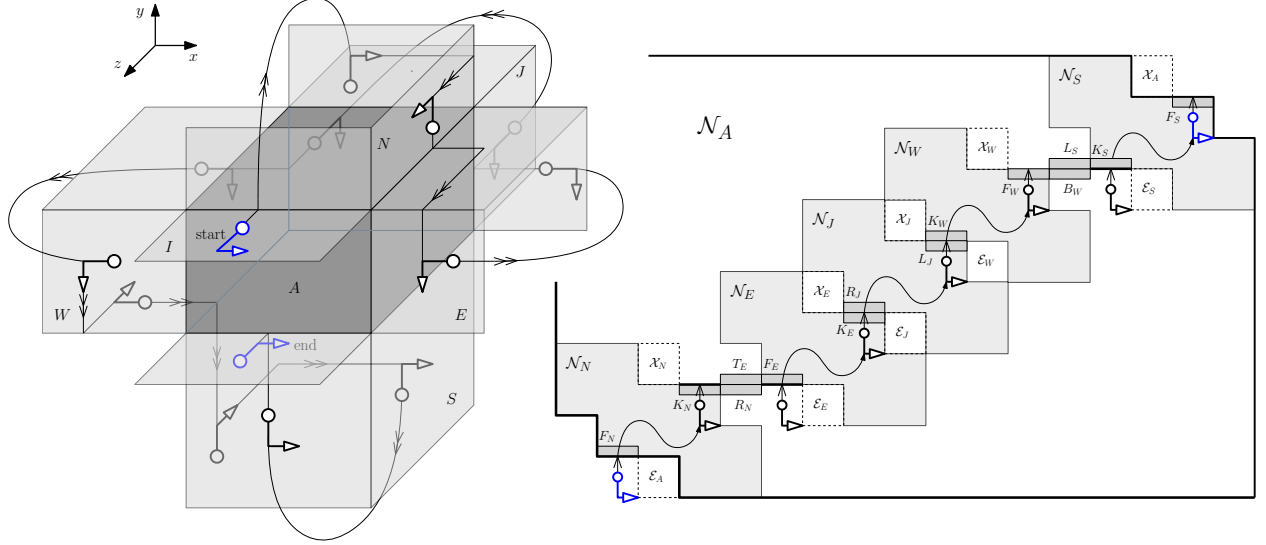


Figure 14: Unfolding of degree-6 box A (a) unfolding path (b) unfolding net \mathcal{N}_A .

Theorem 7. *Let $A \in \mathcal{T}$ be a degree-6 box. If A 's children satisfy invariants (I1)-(I3), then A satisfies invariants (I1)-(I3).*

Proof. Consider the unfolding depicted in Figure 14. Observe that it is a generalization of the degree-5 unfolding from Figure 12, where the unfolded face K_A is replaced by the recursive unfolding of child J . This generalization is possible because N and S are non-junctions by Proposition 14. Since the two unfoldings and their proofs are very similar, we only point out the differences here.

We first note that all children of A provide type-1 entry and exit connectors, since they are all leaves or connector boxes by Proposition 14, and the unfoldings for these types of boxes use only type-1 connectors. In

particular, this means that the type-1 exit connector $x'_E \in K_E$ of \mathcal{N}_E connects to the type-1 entry connector $e'_J \in R_J$ of \mathcal{N}_J , as shown in Figure 14. It also means that the type-1 exit connector $x'_J \in L_J$ of \mathcal{N}_J connects to the type-1 entry connector $e'_W \in K_W$ of \mathcal{N}_W , also shown in Figure 14. Thus \mathcal{N}_A is connected.

Applying arguments similar to those in Lemma 13 and noting that \mathcal{N}_J includes all open faces in \mathcal{T}_J with 4×4 refinement (by invariant (II) applied to J), we conclude that the net \mathcal{N}_A from Figure 11 satisfies invariants (I1)-(I3). \square

8 Complete Unfolding Example

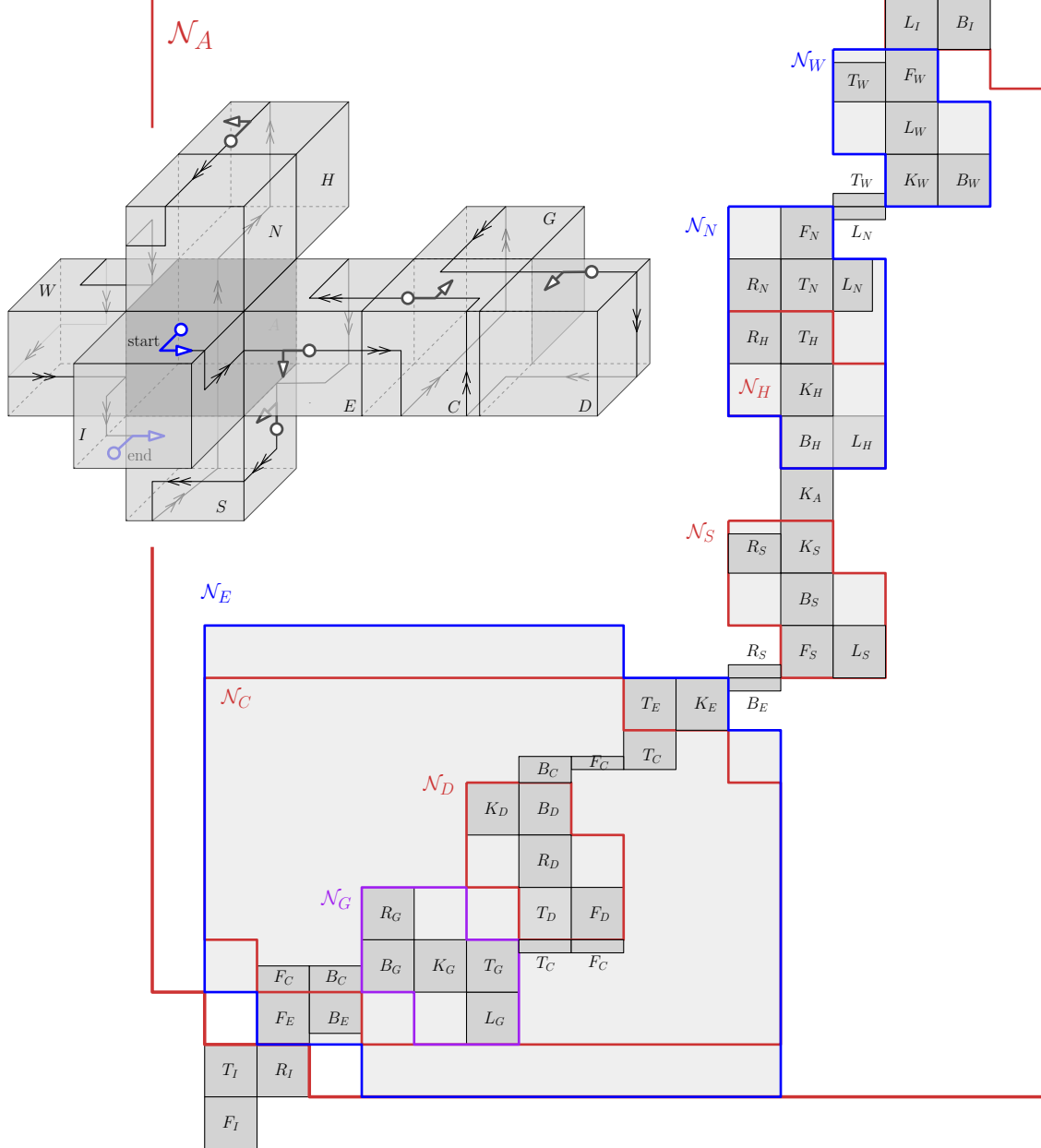


Figure 15: Complete unfolding example of a polycube tree (with root I). Here C is the box that requires a 4-refinement along one grid dimension.

Figure 15 illustrates a complete unfolding example for a polycube tree composed of ten boxes. The root I of the unfolding tree \mathcal{T} is a degree-1 box with back child A , which is unfolded recursively. Observe that A is a degree-5 box with non-junction children E and W , therefore its unfolding follows the pattern from Figure 13 (which employs the unfolding from Figure 12 in constructing \mathcal{N}'_A). In the following we classify the nodes in \mathcal{T} based on their degree and orientation, and map them to the unfolding patterns discussed in earlier sections. To be able to do so, we view each node in \mathcal{T} in standard position (with parent attached to the front face and entry and exit ports on top and bottom edges of the front face, respectively):

- The east child E of A is a degree-2 box with back child C , so its unfolding follows the pattern from Figure 8a.
- C is a degree-3 box with back child D and south child G , so its unfolding follows the pattern from Figure 10a, traversed in reverse.
- N is a degree-2 box with north child H , so its unfolding follows the pattern from Figure 8b.
- D , S , H and W are leaves that employ the HEAD-first unfolding pattern from Figure 2a.
- G is a leaf that uses the HAND-first unfolding pattern from Figure 2b.

The result is the net depicted in Figure 15, with the subnets marked and appropriately labeled.

9 Conclusion

We show that every polycube tree can be unfolded with a 4×4 refinement of the grid faces. This is the first result on unfolding arbitrary polycube trees using a constant refinement of the grid. It is open whether all polycube trees can be grid-unfolded without any refinements.

References

- [BDD⁹⁸] Therese Biedl, Erik Demaine, Martin Demaine, Anna Lubiw, Mark Overmars, Joseph O'Rourke, Steve Robbins, and Sue Whitesides. Unfolding some classes of orthogonal polyhedra. In *Proceedings of the 10th Canadian Conference on Computational Geometry*, Montréal, Canada, August 1998.
- [BDE⁰³] Marshall Bern, Erik Demaine, David Eppstein, Eric Kuo, Andrea Mantler, and Jack Snoeyink. Ununfoldable polyhedra with convex faces. *Computational Geometry: Theory and Applications*, 24(2):51–62, February 2003.
- [CY15] Yi-Jun Chang and Hsu-Chun Yen. Unfolding orthogonal polyhedra with linear refinement. In *Proceedings of the 26th International Symposium on Algorithms and Computation, ISAAC 2015, Nagoya, Japan*, pages 415–425. Springer Berlin Heidelberg, 2015.
- [DDF14] Mirela Damian, Erik Demaine, and Robin Flatland. Unfolding orthogonal polyhedra with quadratic refinement: the Delta-unfolding algorithm. *Graphs and Combinatorics*, 30(1):125–140, 2014.
- [DDFO17] Mirela Damian, Erik Demaine, Robin Flatland, and Joseph O'Rourke. Unfolding genus-2 orthogonal polyhedra with linear refinement. *Graph. Comb.*, 33(5):1357–1379, September 2017.
- [DF18] Mirela Damian and Robin Flatland. Unfolding low-degree orthotrees with constant refinement. In *Proceedings of the 30th Canadian Conference on Computational Geometry*, pages 189–208, Winnipeg, Canada, August 2018.
- [DFMO05] Mirela Damian, Robin Flatland, Henk Meijer, and Joseph O'Rourke. Unfolding well-separated orthotrees. In *Abstracts from the 15th Annual Fall Workshop on Computational Geometry*, Philadelphia, PA, November 2005.

- [DFO05] Mirela Damian, Robin Flatland, and Joseph O'Rourke. Unfolding Manhattan towers. In *Proceedings of the 17th Canadian Conference on Computational Geometry*, pages 211–214, Windsor, Canada, August 2005.
- [DFO07] Mirela Damian, Robin Flatland, and Joseph O'Rourke. Epsilon-unfolding orthogonal polyhedra. *Graphs and Combinatorics*, 23(1):179–194, 2007.
- [DO07] Erik Demaine and Joseph O'Rourke. *Geometric Folding Algorithms: Linkages, Origami, Polyhedra*. Cambridge University Press, July 2007.
- [HCY17] Kuan-Yi Ho, Yi-Jun Chang, and Hsu-Chun Yen. Unfolding some classes of orthogonal polyhedra of arbitrary genus. In *The 23th International Computing and Combinatorics Conference (COCOON) 2017*, pages 275–287, 2017.
- [LPW14] Meng-Huan Liou, Sheung-Hung Poon, and Yu-Jie Wei. On edge-unfolding one-layer lattice polyhedra with cubic holes. In *The 20th International Computing and Combinatorics Conference (COCOON) 2014*, pages 251–262, 2014.

A Unfolding Degree-3 Nodes (Remaining Cases)

This and subsequent appendices discuss unfoldings for cases not included in the main body of the paper. We illustrate the unfolding path and the resulting unfolding net for each case scenario, then present a digest of the correctness proof that focuses on the specifics of each case. When combined with arguments similar to the ones used in the main part of the paper, each proof digest yields a complete correctness proof. This way we avoid repetition and improve the readability flow.

In this section we discuss the unfoldings for cases 3.3 through 3.6 listed in Section 7.2.

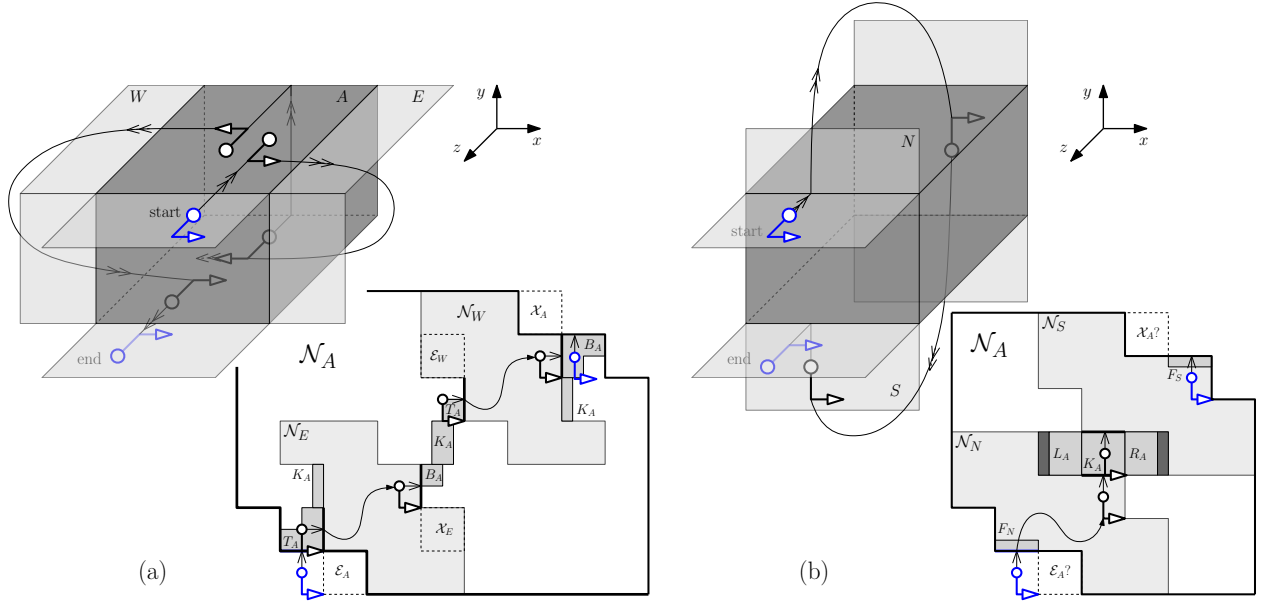


Figure 16: Unfolding degree-3 box A with parent I (a) children E and W (b) children N and S.

Lemma 15. *Let $A \in \mathcal{T}$ be a degree-3 node with parent I and children E and W (Case 3.3). If A's children satisfy invariants (I1)-(I3), then A satisfies invariants (I1)-(I3).*

Proof. Consider the unfolding from Figure 16a, and notice that this unfolding is a degenerate case of the unfolding from Figure 11, where the recursive unfolding of the child J is replaced by the face K_A . Since the two unfoldings and their proofs of correctness are very similar, we only point out the differences here:

- Since $\xrightarrow{e_E} \in K_A$ is open and adjacent to T_E , the unit square \mathcal{E}_E (occupied by $\xrightarrow{e_E}$ in Figure 16a) does not belong to the inductive region for E and \mathcal{N}_E may provide a type-1 or a type-2 entry connection: if type-1, it connects to the ring face $e_E \in T_A$ placed alongside its entry port (as in the general case from Figure 11); if type-2, it connects to the ring face $\xrightarrow{e_E} \in K_A$ placed alongside its entry port extension.
- Similarly, since $\xleftarrow{x_W} \in K_A$ is open and adjacent to T_W , the unit square \mathcal{X}_W (occupied by $\xleftarrow{x_W}$ in Figure 16a) does not belong to the inductive region for W and \mathcal{N}_W may provide a type-1 or a type-2 exit connection: if type-1, it connects to the ring face $x_W \in B_A$ placed alongside its exit port (as in the general case from Figure 11); if type-2, it connects to the ring face $\xleftarrow{x_W} \in K_A$ placed alongside its exit port extension.

These changes are reflected in Figure 16a. Arguments similar to the ones used in the proof of Lemma 11 show that the net \mathcal{N}_A from Figure 16a satisfies invariants (I1)-(I3). \square

Lemma 16. *Let $A \in \mathcal{T}$ be a degree-3 node with parent I and children N and S (Case 3.4). If A's children satisfy invariants (I1)-(I3), then A satisfies invariants (I1)-(I3).*

Proof. Consider the unfolding from Figure 16b, and notice that it is a generalization of the unfolding from Figure 8b, where the unfolded face B_A is replaced by the recursive unfolding of S . Since the two unfoldings and their proofs of correctness are very similar, we only point out the differences here:

- The entry and exit ring faces for S are $e_S \in K_A$ and $x_S \in B_I$, respectively.
- Since $\xrightarrow{e_S} \in R_A$ is open and adjacent to T_S , the unit square \mathcal{E}_S (occupied by R_A in Figure 16b) does not belong to the inductive region for S and \mathcal{N}_S may provide a type-1 or a type-2 entry connection: if type-1, it connects to the ring face $e_S \in K_A$ placed alongside its entry port; if type-2, it connects to the ring face $\xrightarrow{e_S} \in R_A$ placed alongside its entry port extension.
- Since $\xleftarrow{x_S} \in L_I$ is not adjacent to T_S , \mathcal{N}_S will provide a type-1 exit connection, which is also a type-1 exit connection for \mathcal{N}_A (because $x_S = x_A$).

These observations, along with the arguments used in the proof of Lemma 8, show that the unfolding \mathcal{N}_A from Figure 16b satisfies invariants (I1)-(I3). \square

Lemma 17. *Let $A \in \mathcal{T}$ be a degree-3 node with parent I and children N and E (Case 3.5). If A 's children satisfy invariants (I1)-(I3), then A satisfies invariants (I1)-(I3).*

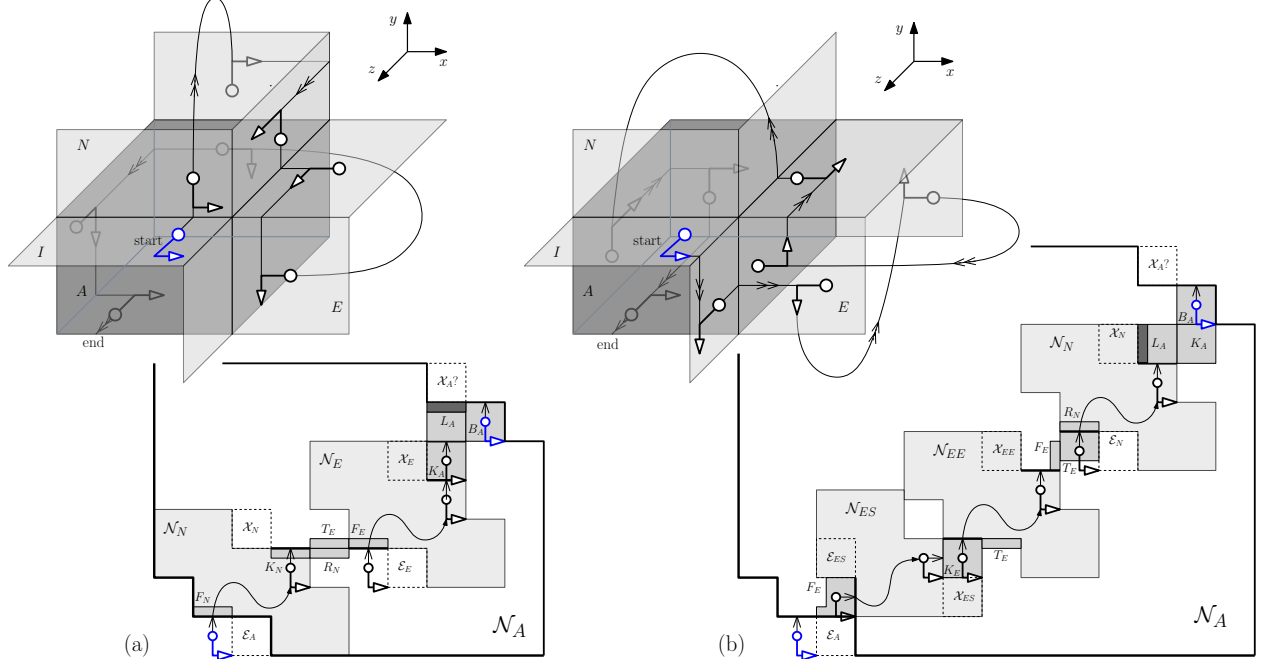


Figure 17: HAND-east unfolding of degree-3 box A with parent I and children N and E (a) K_N open (b) K_N closed (so K_E open); unfolding shown for case when ES and EE exist.

Proof. We discuss two different scenarios, depending on whether K_N is open or closed. Assume first that K_N is open, and consider the HAND-east unfolding depicted in Figure 17a. Notice that this unfolding follows a path very similar to the one from Figure 12 (which depicts the case where A has two additional children W and S), so in a way this case can be viewed as a degenerate case of the one from Figure 12. The only difference is that, in Figure 17a, once the unfolding path reaches the back face K_A , it continues HEAD-first to L_A and then HAND-first to the exit port of A . Note that the resulting net \mathcal{N}_A provides a type-1 exit connection $x'_A \in B_A$, and the ring face $\xleftarrow{x'_A} \in L_A$ (dark-shaded in Figure 17a) can be removed from \mathcal{N}_A without disconnecting \mathcal{N}_A . These observations, combined with the arguments used in the proof of Lemma 13, show that \mathcal{N}_A satisfies invariants (I1)-(I3).

Assume now that K_N is closed (note that in this case K_E is open), and consider the HAND-east unfolding depicted in Figure 17b, which handles the more general case where ES and EE exist (handling cases when one or both of these boxes are missing requires only minor modifications). Note that $\xrightarrow{e_A} \in R_I$ is open and adjacent to \mathcal{T}_A , and \mathcal{N}_A provides a type-2 entry connection $\xrightarrow{e'_A} \in F_E$. Also note that \mathcal{N}_A provides a type-1 exit connection $\xrightarrow{x'_A} \in B_E$. These together show that \mathcal{N}_A satisfies invariant (I2). The following observations support our claim that \mathcal{N}_A satisfies invariant (I1):

- The entry and exit ring faces for ES , EE and N are as follows: $e_{ES} \in F_E$ and $x_{ES} \in K_E$; $e_{EE} \in K_E$ and $x_{EE} \in F_E$; and $e_N \in T_E$ and $x_N \in L_A$.
- \mathcal{N}_{ES} and \mathcal{N}_N provide type-1 entry connections. This is because $\xrightarrow{e_{ES}} \in R_E$ is closed, and $\xrightarrow{e_N} \in K_E$ is not adjacent to \mathcal{T}_E .
- Since $\xrightarrow{e_{EE}} \in T_E$ is open, the unit square \mathcal{E}_{EE} (occupied by $\xrightarrow{e_{EE}}$ in Figure 17b) does not belong to the inductive region for EE .
- \mathcal{N}_{ES} , \mathcal{N}_{EE} and \mathcal{N}_N provide type-1 exit connections. This is because $\xleftarrow{x_{ES}} \in L_E$, $\xleftarrow{x_{EE}} \in B_E$ and $\xleftarrow{x_N} \in F_A$ are all closed.

Regarding invariant (I3), note that the open ring face of A located on L_A (dark-shaded in Figure 17b) can be removed from \mathcal{N}_A without disconnecting \mathcal{N}_A , therefore \mathcal{N}_A satisfies (I3). \square

Lemma 18. *Let $A \in \mathcal{T}$ be a degree-3 node with parent I and children N and W (Case 3.6). If A 's children satisfy invariants (I1)-(I3), then A satisfies invariants (I1)-(I3).*

Proof. This case is slightly more complex and spans four different case scenarios:

1. B_I open
2. T_N open
3. B_I closed, T_N closed and K_N open
4. B_I closed, T_N closed and K_N closed

Case 1: B_I open. Consider the unfolding depicted in Figure 18a, and identify the following entry and exit ring faces for N and W : $e_N \in T_I$ and $x_N \in K_A$; and $e_W \in B_A$ and $x_W \in L_N$. Note that $\xrightarrow{e_N} \in R_I$ is not adjacent to \mathcal{T}_N , therefore \mathcal{N}_N provides a type-1 entry connection $\xrightarrow{e'_N} \in F_N$, which is also a type-1 entry connection for \mathcal{N}_A (since $e_A = e_N$). Also note that $\xleftarrow{x_A} \in L_I$ is open and adjacent to \mathcal{T}_A , and \mathcal{N}_A provides a type-2 exit connection $\xleftarrow{x'_A} \in F_W$. These together show that \mathcal{N}_A satisfies invariant (I2). Turning to (I1), note that \mathcal{N}_N and \mathcal{N}_W provide type-1 entry and exit connections. This is because $\xleftarrow{x_N} \in L_A$ is closed, $\xrightarrow{e_W} \in F_A$ is closed, and $\xleftarrow{x_W} \in K_N$ is not adjacent to \mathcal{T}_W . These together imply that \mathcal{N}_A satisfies invariant (I1). Finally, note that the ring face of A located on R_A (dark-shaded in Figure 18a) can be removed without disconnecting \mathcal{N}_A , so \mathcal{N}_A satisfies invariant (I3) as well.

Case 2: T_N open. Consider the unfolding depicted in Figure 18b, which handles the more general case where NE and NJ exist (handling cases when one or both of these boxes are missing requires only minor modifications). Note that \mathcal{N}_A provides type-1 entry and exit connections $e'_A \in F_N$ and $x'_A \in B_A$, therefore \mathcal{N}_A satisfies invariant (I2). The following observations support our claim that \mathcal{N}_A satisfies invariant (I1):

- The entry and exit ring faces for NE , NJ and W are as follows: $e_{NE} \in T_N$ and $x_{NE} \in R_A$; $e_{NJ} \in K_A$ and $x_{NJ} \in T_N$; and $e_W \in L_N$ and $x_W \in B_A$.
- \mathcal{N}_{NE} , \mathcal{N}_{NJ} and \mathcal{N}_W provide type-1 entry connections. This is because $\xrightarrow{e_{NE}} \in K_N$ and $\xrightarrow{e_{NJ}} \in L_A$ are closed, and $\xrightarrow{e_W} \in F_N$ is not adjacent to \mathcal{T}_W .
- \mathcal{N}_{NE} and \mathcal{N}_{NJ} provide type-1 exit connections, since $\xleftarrow{x_{NE}} \in F_A$ and $\xleftarrow{x_{NJ}} \in R_N$ are closed.

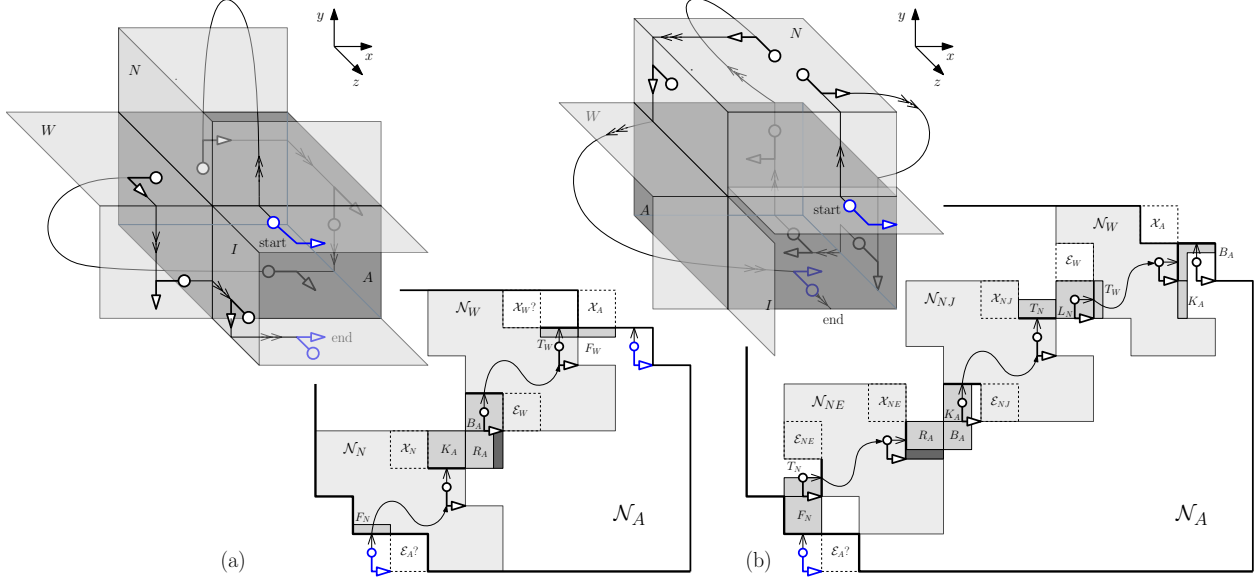


Figure 18: Unfolding of degree-3 box A with parent I and children N and W (a) B_I open (b) T_N open; unfolding shown for the case when NE and NJ exist.

- Since $\xleftarrow{x_W} \in K_A$ is open, the unit square X_W (occupied by $\xleftarrow{x_W}$ in Figure 18b) does not belong to the inductive region for W .

Arguments similar to the ones above show that \mathcal{N}_A satisfies invariant (I3) as well.

Case 3: B_I, T_N closed and K_N open. Note that in this case B_W is open. Consider the unfolding depicted in Figure 19, which handles the more general case where NE , WW and WJ exist (handling cases when one or more of these boxes do not exist requires only minor modifications). Arguments similar to the ones above show that \mathcal{N}_A satisfies invariants (I2) and (I3). The following observations support our claim that \mathcal{N}_A satisfies invariant (I1):

- The entry and exit ring faces for NE , NN , WW and WJ are as follows: $e_{NE} \in F_N$ and $x_{NE} \in K_N$; $e_{NN} \in K_N$ and $x_{NN} \in F_N$; $e_{WW} \in B_W$ and $x_{WW} \in T_W$; and $e_{WJ} \in T_W$ and $x_{WJ} \in B_W$.
- \mathcal{N}_{NE} , \mathcal{N}_{WW} and \mathcal{N}_{WJ} provide type-1 entry connections, since $\xrightarrow{e_{NE}} \in T_N$, $\xrightarrow{e_{WW}} \in K_W$ and $\xrightarrow{e_{WJ}} \in R_W$ are closed. Since $\xrightarrow{e_{NN}} \in L_N$ is open, the unit square E_{NN} (occupied by $\xrightarrow{e_{NN}}$ in Figure 19) does not belong to the inductive region for NN .
- \mathcal{N}_{NE} , \mathcal{N}_{NN} and \mathcal{N}_{WJ} provide type-1 exit connections, since $\xleftarrow{x_{NE}} \in B_N$, $\xleftarrow{x_{NN}} \in R_N$ and $\xleftarrow{x_{WJ}} \in L_W$ are closed. Since $\xleftarrow{x_{WW}} \in F_W$ is open, the unit square X_{WW} (occupied by $\xleftarrow{x_{WW}}$ in Figure 19) does not belong to the inductive region for WW .

Case 4: B_I , T_N and K_N closed. Note that in this case NJ exists, and T_{NJ} and L_{NJ} are open. Consider the unfolding depicted in Figure 20, which handles the more general case where NE exists (handling the case when NE does not exist requires only minor modifications). Arguments similar to the ones above show that \mathcal{N}_A satisfies invariants (I2) and (I3). The following observations support our claim that \mathcal{N}_A satisfies invariant (I1):

- The entry and exit ring faces for NE , NJ , NN and W are as follows: $e_{NE} \in F_N$ and $x_{NE} \in R_{NJ}$; $e_{NJ} \in K_{NE}$ and $x_{NJ} \in L_N$; $e_{NN} \in T_{NJ}$ and $x_{NN} \in F_N$; and $e_W \in L_N$ and $x_W \in B_A$.
- \mathcal{N}_{NE} , \mathcal{N}_{NJ} , \mathcal{N}_{NN} and \mathcal{N}_W provide type-1 entry connections. This is because $\xrightarrow{e_{NE}} \in T_N$ is closed, $\xrightarrow{e_{NJ}} \in T_{NE}$ is not adjacent to T_{NJ} , $\xrightarrow{e_{NN}} \in R_{NJ}$ is not adjacent to T_{NN} , and $\xrightarrow{e_W} \in F_N$ is not adjacent to T_W .

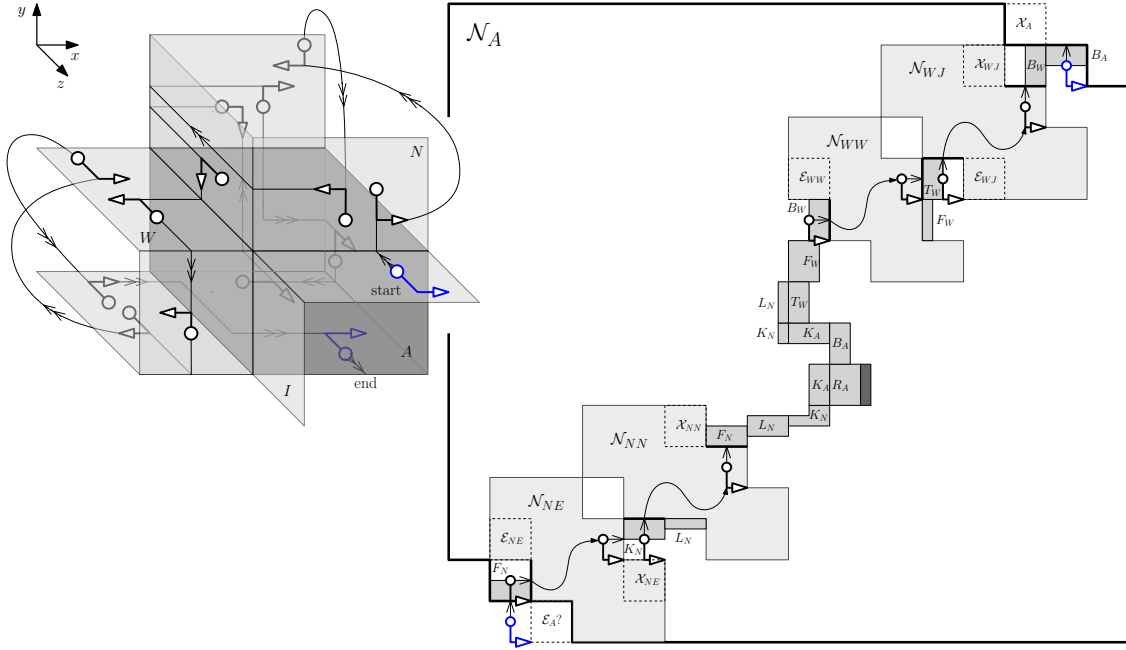


Figure 19: Unfolding of degree-3 box \$A\$ with parent \$I\$ and children \$N\$ and \$W\$, case \$B_I\$ closed (so \$B_W\$ open), \$T_N\$ closed and \$K_N\$ open.

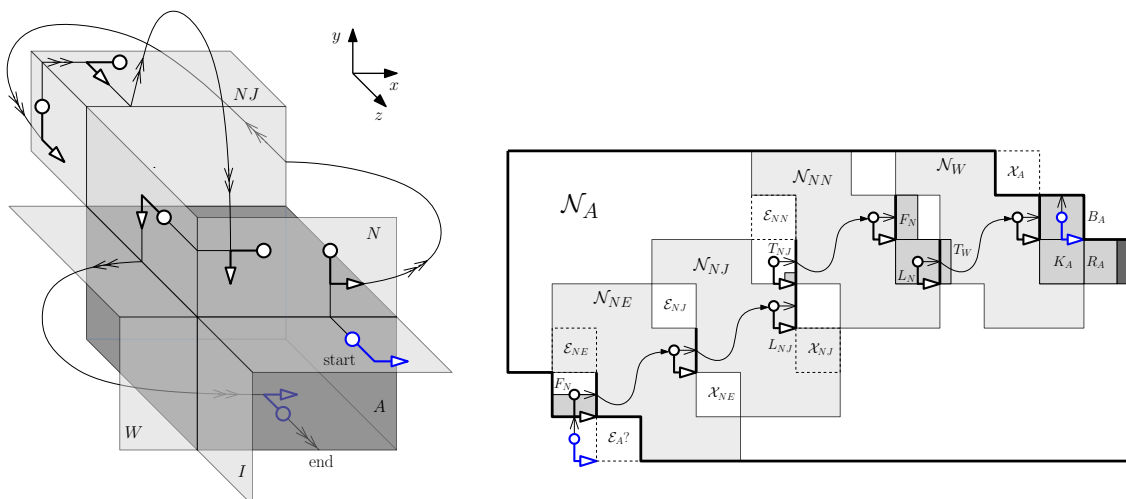


Figure 20: Unfolding of degree-3 box \$A\$ with parent \$I\$ and children \$N\$ and \$E\$, case \$B_I\$ closed (so \$B_W\$ open), \$T_N\$ closed and \$K_N\$ closed (and so \$T_{NJ}\$ and \$L_{NJ}\$ open).

- \mathcal{N}_{NE} and \mathcal{N}_{NJ} provide type-1 exit connections. This is because $\xleftarrow{x_{NE}} \in B_{NJ}$ is not adjacent to \mathcal{T}_{NE} , and $\xleftarrow{x_{NJ}} \in B_N$ is closed. Note that the type-1 exit connection of \mathcal{N}_{NE} connects to the type-1 entry connection of \mathcal{N}_{NJ} .
- Since $\xleftarrow{x_{NN}} \in L_N$ is open, the unit square \mathcal{X}_{NN} (occupied by L_N in Figure 20) does not belong to the inductive region for NN .
- Similarly, since $\xleftarrow{x_W} \in K_A$ is open, the unit square \mathcal{X}_W (occupied by K_A in Figure 20) does not belong to the inductive region for W .
- By invariant (I3) applied to NJ , the ring face that lies on T_{NJ} (not used in the entry or exit connections for NJ) can be relocated outside of \mathcal{N}_{NJ} . In Figure 20, we use a piece of T_{NJ} to connect \mathcal{N}_{NJ} and \mathcal{N}_{NN} together.

Having exhausted all possible cases, we conclude that this lemma holds. \square

B Unfolding Degree-4 Nodes (Remaining Cases)

In this section we discuss the unfoldings for cases 4.2 through 4.7 listed in Section 7.3.

Lemma 19. *Let $A \in \mathcal{T}$ be a degree-4 node with parent I and children N, E , and W (Case 4.2). If A 's children satisfy invariants (I1)-(I3), then A satisfies invariants (I1)-(I3).*

Proof. We discuss the following three exhaustive scenarios:

1. K_N closed
2. K_N open and B_I closed
3. K_N open and B_I open

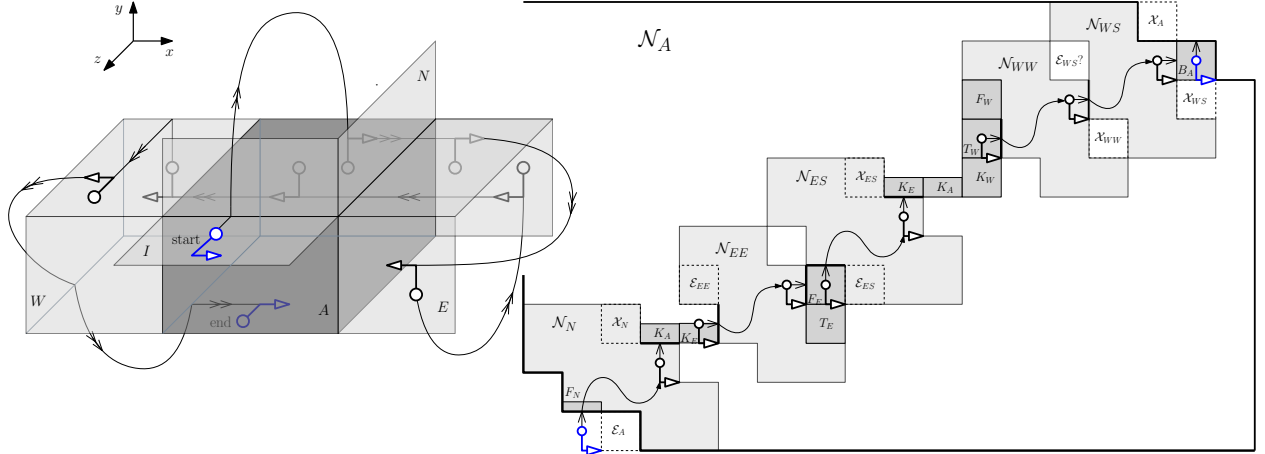


Figure 21: Unfolding of degree-4 box A with N, E and W children, case K_N closed (so K_E, K_W open); unfolding shown for the case when EE, ES, WW and WS exist.

Case 1: K_N closed. It can be easily verified that in this case K_E and K_W are open. Consider the unfolding depicted in Figure 21, which handles the more general case where EE, ES, WW and WS exist (handling cases when one or more of these boxes do not exist requires only minor modifications). Note that \mathcal{N}_A provides a type-1 entry connection (by arguments similar to the ones used in the proof of Lemma 13) and a type-1 exit connection $x'_A \in B_A$, therefore \mathcal{N}_A that satisfies invariant (I2). Also note that the only open ring face of A is the exit ring face, so \mathcal{N}_A trivially satisfies (I3). The following observations support our claim that \mathcal{N}_A is connected and satisfies invariant (I1):

- The entry and exit ring faces for N , EE , ES , WW and WS are as follows: $e_N \in T_I$ and $x_N \in K_A$; $e_{EE} \in K_E$ and $x_{EE} \in F_E$; $e_{ES} \in F_E$ and $x_{ES} \in K_E$; $e_{WW} \in T_W$ and $x_{WW} \in L_{WS}$; and $e_{WS} \in B_{WW}$ and $x_{WS} \in B_A$.
- \mathcal{N}_N , \mathcal{N}_{ES} , \mathcal{N}_{WW} and \mathcal{N}_{WS} provide type-1 exit connections. This is because $\xleftarrow{x_N} \in L_A$ is closed, $\xleftarrow{x_{ES}} \in R_E$ is closed, $\xleftarrow{x_{WW}} \in K_{WS}$ is not adjacent to \mathcal{T}_{WW} , and $\xleftarrow{x_{WS}} \in K_A$ is open but not adjacent to \mathcal{T}_{WS} .
- \mathcal{N}_{EE} , \mathcal{N}_{ES} and \mathcal{N}_{WS} provide type-1 entry connections. This is because $\xrightarrow{e_{EE}} \in B_E$ is closed (since ES exists), $\xrightarrow{e_{ES}} \in L_E$ is closed, and $\xrightarrow{e_{WS}} \in F_{WW}$ is not adjacent to \mathcal{T}_{WS} . Note that the type-1 entry connection of \mathcal{N}_{WS} connects to the type-1 exit connection of \mathcal{N}_{WW} .
- Since $\xleftarrow{x_{EE}} \in T_E$ is open, the unit square \mathcal{X}_{EE} (occupied by T_E in Figure 21) does not belong to the inductive region for EE .
- Since $\xrightarrow{e_{WW}} \in F_W$ is open, the unit square \mathcal{E}_{WW} (occupied by F_W in Figure 21) does not belong to the inductive region for WW .

Note that we split the unfolding of W into two subnets (\mathcal{N}_{WW} and \mathcal{N}_{WS}) so as to avoid sharing the ring face on K_W between its current position in \mathcal{N}_A and the type-2 exit connection that \mathcal{N}_W would have provided (had it not been split). A similar intuition was used to split the unfolding of E into \mathcal{N}_{EE} and \mathcal{N}_{ES} .

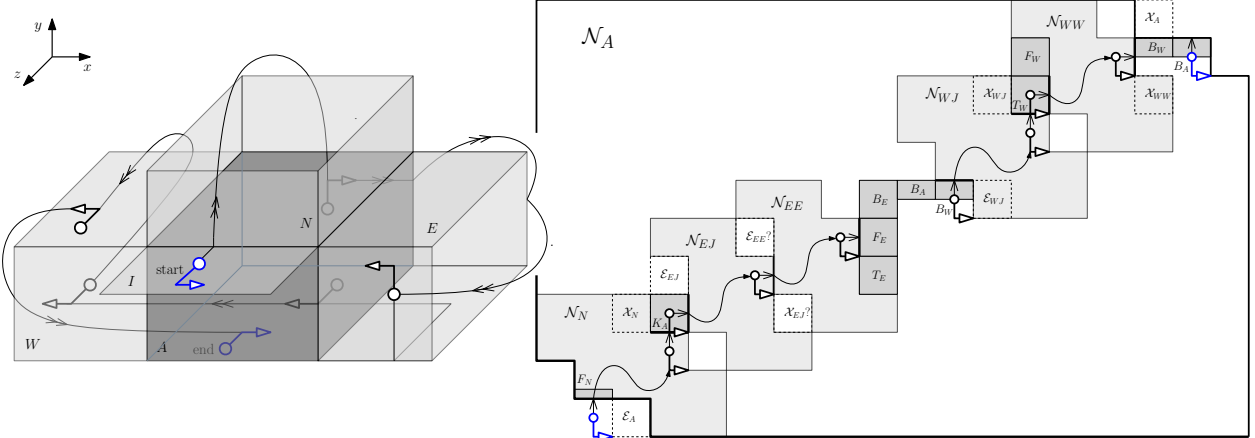


Figure 22: Unfolding of degree-4 box A with N , E and W children, case K_N open and B_I closed (so B_E , B_W open); unfolding shown for the case when EJ , EE , WJ and WW exist.

Case 2: K_N open and B_I closed. In this case B_E and B_W are open (refer to Figure 22, which shows the unfolding for the case when EJ , EE , WJ and WW exist). Arguments similar to ones used in the previous case show that \mathcal{N}_A satisfies invariants (I2) and (I3). The following observations support our claim that \mathcal{N}_A is connected and satisfies invariant (I1):

- Same arguments as in Case 1 apply to the entry and exit ports of \mathcal{N}_N .
- The entry and exit ring faces for EJ , EE , WJ and WW are as follows: $e_{EJ} \in K_A$ and $x_{EJ} \in K_{EE}$; $e_{EE} \in R_{EJ}$ and $x_{EE} \in F_E$; $e_{WJ} \in B_W$ and $x_{WJ} \in T_W$; and $e_{WW} \in T_W$ and $x_{WW} \in B_W$.
- \mathcal{N}_{EJ} provides a type-1 entry connection, since $\xrightarrow{e_{EJ}} \in B_A$ is not adjacent to \mathcal{T}_{EJ} . Also note that $\xleftarrow{x_{EJ}} \in T_{EE}$ is not adjacent to \mathcal{T}_{EE} , therefore \mathcal{N}_{EJ} provides a type-1 exit connection.
- Since $\xrightarrow{e_{EE}} \in B_{EJ}$ is not adjacent to \mathcal{T}_{EE} , \mathcal{N}_{EE} provides a type-1 entry connection (which attaches to the type-1 exit connection of \mathcal{N}_{EJ}). Also, since $\xleftarrow{x_{EE}} \in T_E$ is open, the unit square \mathcal{X}_{EE} (occupied by T_E in Figure 22) does not belong to the inductive region for EE .

- \mathcal{N}_{WJ} provides type-1 entry and exit connections, since $\xrightarrow{e_{WJ}} \in L_W$ is closed (by our assumption that WW exists) and $\xleftarrow{x_{WJ}} \in R_W$ is also closed.
- Since $\xrightarrow{e_{WW}} \in F_W$ is open, the unit square \mathcal{E}_{WW} (occupied by F_W in Figure 22) does not belong to the inductive region for WW .
- Since $\xleftarrow{x_{WW}} \in K_W$ is closed, \mathcal{N}_{WW} provides a type-1 exit connection.

As in the previous case, we split the unfolding of E into two subnets, \mathcal{N}_{EJ} and \mathcal{N}_{EE} , so as to avoid sharing part of A 's exit ring face with the type-2 entry connection that \mathcal{N}_E would have provided (had it not been split).

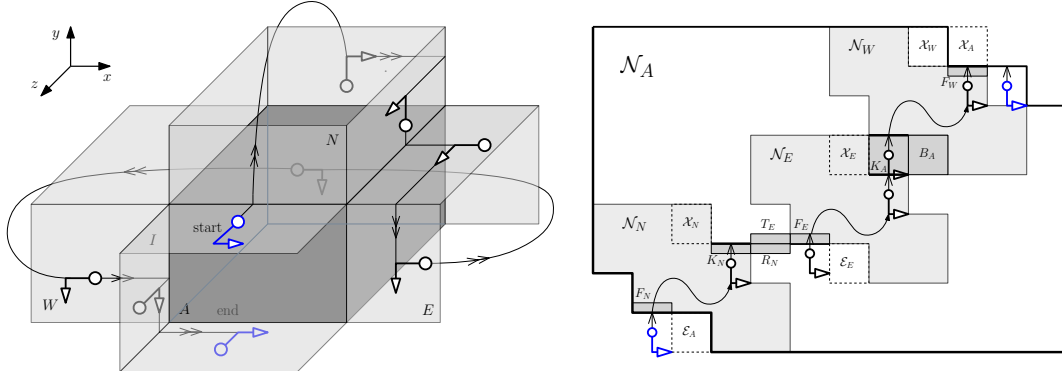


Figure 23: Unfolding of degree-4 box A with N , E and W children, case K_N open and B_I open.

Case 3: K_N open and B_I open. The unfolding for this case is depicted in Figure 23. Note that this unfolding follows a path similar to the one depicted in Figure 17a up to the point where it reaches K_A , where it deviates and proceeds with the recursive unfolding of W . Note that the entry and exit ring faces for W are $e_W \in K_A$ and $x_W \in L_I$.

Observe that $\xleftarrow{x_W} \in T_I$ is open but not adjacent to \mathcal{T}_W , therefore \mathcal{N}_W provides a type-1 exit connection $x'_W \in F_W$, which is a type-2 exit connection for \mathcal{N}_A . This along with the fact that $\xleftarrow{x_A} \in L_I$ is adjacent to \mathcal{T}_A , shows that the exit port of \mathcal{N}_A satisfies invariant (I2). Arguments similar to the ones used in Case 1 above show that the entry port of \mathcal{N}_A also satisfies (I2), and that \mathcal{N}_A satisfies (I3) as well.

Turning to (I1), notice that $\xrightarrow{e_W} \in B_A$ is open, therefore the unit square \mathcal{E}_W (occupied by B_A in Figure 23) does not belong to the inductive region for W . Furthermore, since $\xrightarrow{e_W}$ is adjacent to \mathcal{T}_W , \mathcal{N}_W may provide a type-1 or type-2 entry connection, which attaches to K_A or B_A placed alongside its entry port and entry port extension, respectively. This, along with the arguments used in the proof of Lemma 17 showing that \mathcal{N}_N and \mathcal{N}_E connect together, shows that \mathcal{N}_A is connected and satisfies invariant (I1). \square

Lemma 20. *Let $A \in \mathcal{T}$ be a degree-4 node with parent I and children N , E , and J (Case 4.3). If A 's children satisfy invariants (I1)-(I3), then A satisfies invariants (I1)-(I3).*

Proof. Consider the HAND-east unfolding depicted in Figure 24, and notice that this unfolding is a generalization of the degree-3 unfolding from Figure 17a, where the unfolded face K_A is replaced by the recursive unfolding of child J . Arguments similar to the ones used in the proof of Lemma 17 show that the unfolding \mathcal{N}_A from Figure 24 satisfies invariants (I2) and (I3). The following observations support our claim that \mathcal{N}_A is connected and satisfies invariant (I1):

- \mathcal{N}_N and \mathcal{N}_E are connected (by the proof of Lemma 17).
- \mathcal{N}_E provides a type-1 exit connection, since $\xleftarrow{x_E} \in T_J$ is not adjacent to \mathcal{T}_E . This connection attaches to the type-1 entry connection provided by \mathcal{N}_J (since $\xrightarrow{e_J} \in B_E$ is not adjacent to \mathcal{T}_J). Also, \mathcal{N}_J provides type-1 exit connection (since $\xleftarrow{x_J} \in T_A$ is closed), which attaches to the exit ring face $x_J \in L_A$ placed alongside its exit port.

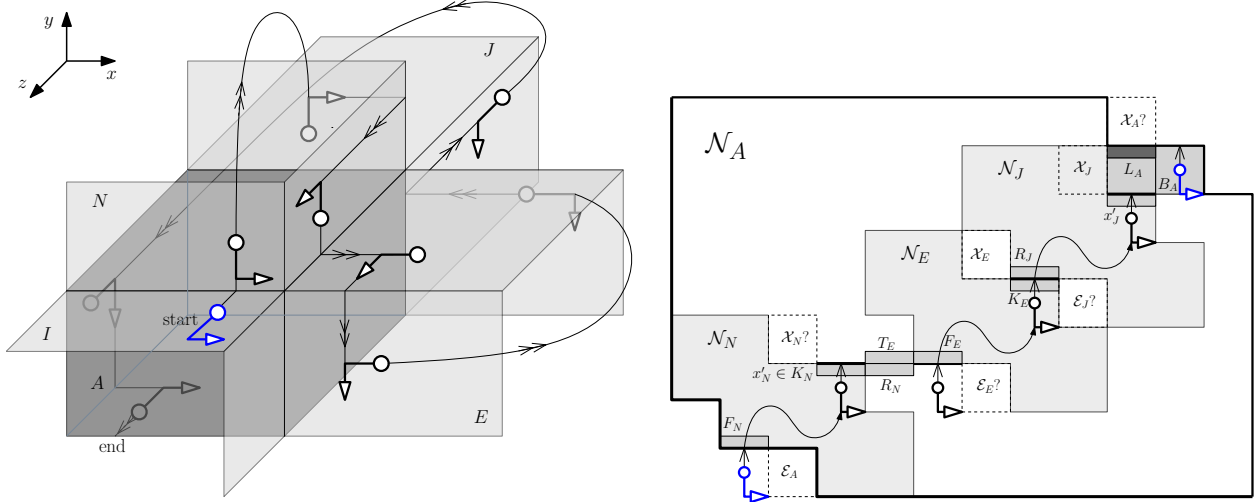


Figure 24: HAND-east unfolding of degree-4 box A with N , E and J children.

This concludes the proof. \square

Lemma 21. *Let $A \in \mathcal{T}$ be a degree-4 node with parent I and children N , W , and J (Case 4.4). If A 's children satisfy invariants (I1)-(I3), then A satisfies invariants (I1)-(I3).*

Proof. The unfolding for this case is slightly more complex and involves four exhaustive scenarios:

1. R_J open
2. R_J closed and R_I closed
3. R_J closed, R_I open and B_J open
4. R_J closed, R_I open and B_J closed

Case 1: R_J open. An unfolding for this case is depicted in Figure 25, which handles the more general case where NE , NN , WW and WS exist (handling cases where one or more of these boxes do not exist requires only minor modifications). First note that \mathcal{N}_A provides a type-1 entry connection $e'_A \in F_N$ and a type-1 exit connection $x'_A \in B_A$, therefore it satisfies invariant (I2). The following observations support our claim that \mathcal{N}_A satisfies invariant (I1):

- The entry and exit ring faces for NE , NN , WW , WS and JJ are as follows: $e_{NE} \in F_N$ and $x_{NE} \in K_N$; $e_{NN} \in K_N$ and $x_{NN} \in F_N$; $e_{WW} \in K_W$ and $x_{WW} \in F_W$; $e_{WS} \in F_W$ and $x_{WS} \in K_W$; and $e_{JJ} \in T_J$ and $x_{JJ} \in B_J$ (which is open, since we assume that B_W is closed).
- \mathcal{N}_{NE} , \mathcal{N}_{WW} and \mathcal{N}_{WS} provide type-1 entry connections. This is because $\xrightarrow{e_{NE}} \in T_N$ is closed (since NN exists), $\xrightarrow{e_{WW}} \in B_W$ is closed, and $\xrightarrow{e_{WS}} \in R_W$ is closed.
- Since $\xrightarrow{e_{NN}} \in L_N$ is open, the unit square \mathcal{E}_{NN} (occupied by $\xrightarrow{e_{NN}}$ in Figure 25) does not belong to the inductive region for NN .
- Since $\xrightarrow{e_{JJ}} \in R_J$ is open, the unit square \mathcal{E}_{JJ} (occupied by R_J in Figure 25) does not belong to the inductive region for JJ . Notice that we place R_A right underneath it.
- \mathcal{N}_{NE} , \mathcal{N}_{NN} and \mathcal{N}_{WS} provide type-1 exit connections. This is because $\xleftarrow{x_{NE}} \in B_N$ is closed, $\xleftarrow{x_{NN}} \in R_N$ is closed (since NE exists), and $\xleftarrow{x_{WS}} \in L_W$ is closed (since WW exists).
- Since $\xleftarrow{x_{WW}} \in T_W$ is open, the unit square \mathcal{X}_{WW} (occupied by $\xleftarrow{x_{WW}}$ in Figure 25) does not belong to the inductive region for WW .

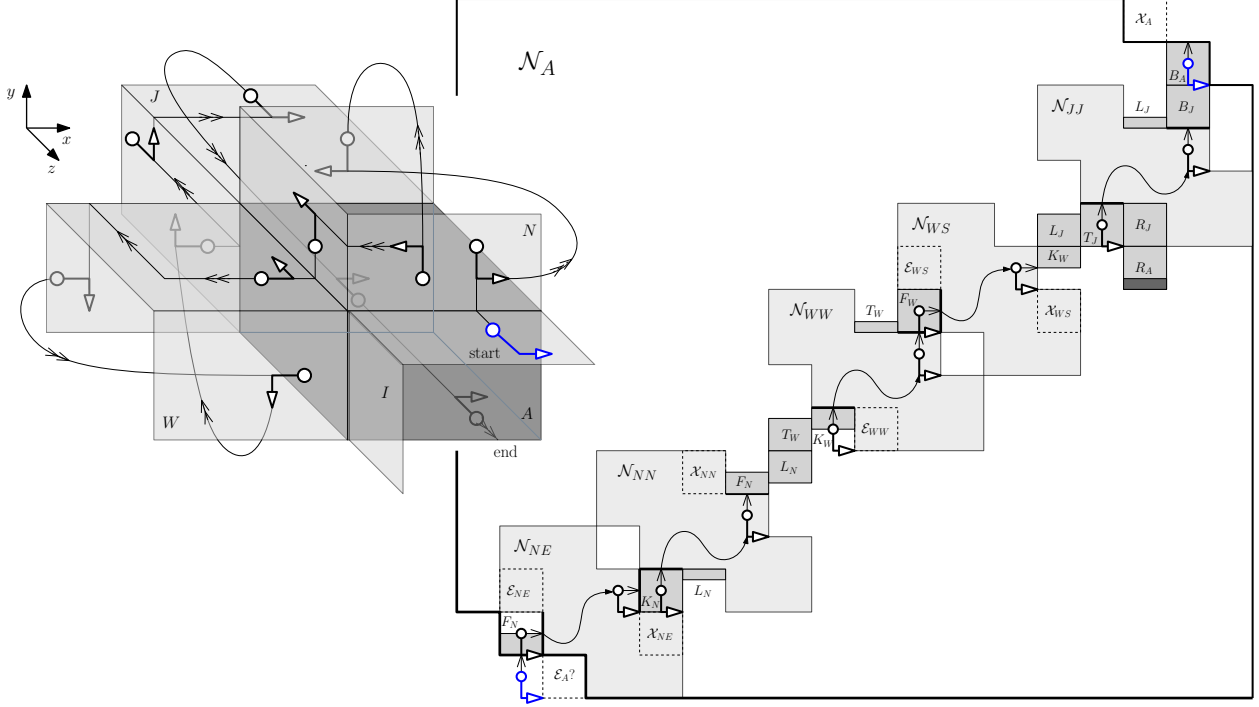


Figure 25: Unfolding for box A of degree 4 with N , W and J children, case R_J open; unfolding shown for general case when NE , NN , WW and WS exist.

- Since $\xleftarrow{x_{JJ}} \in L_J$ is open, the unit square \mathcal{X}_{JJ} (occupied by $\xleftarrow{x_{JJ}}$ in Figure 25) does not belong to the inductive region for JJ .

Turning to invariant (I3), observe that the ring face $\xrightarrow{x'_A} \in R_A$ (dark-shaded in Figure 25) can be removed from \mathcal{N}_A without disconnecting \mathcal{N}_A , so (I3) is met.

Case 2: R_J and R_I closed. An unfolding for this case is depicted in Figure 26. Note that this unfolding is very similar to the one shown in Figure 25, with only a few minor modifications:

- R_N is open, so \mathcal{N}_{NE} reduces to a single face R_N . Since R_I is closed, \mathcal{E}_A belongs to the inductive region for A , therefore we can place R_A underneath R_N .
- From R_N we proceed directly to recursively unfold NN , and in this case $e_{NN} \in R_N$ and $x_{NN} \in L_N$. Since $\xrightarrow{e_{NN}} \in K_N$ is open, the unit square \mathcal{E}_{NN} (occupied by K_N in Figure 26) does not belong to the inductive region for NN . Similarly, since $\xleftarrow{x_{NN}} \in F_N$ is open, the unit square \mathcal{X}_{NN} (occupied by $\xleftarrow{x_{NN}}$ in Figure 26) does not belong to the inductive region for NN .
- The entry and exit ring faces for J are $e_J \in K_N$ and $x_J \in B_A$. Since $\xrightarrow{e_J} \in R_N$ is not adjacent to T_J , and since $\xleftarrow{x_J} \in L_A$ is closed, \mathcal{N}_J provides type-1 entry and exit connections. By invariant (I3), ring face L_J can be removed from \mathcal{N}_J and used as bridge to connect to K_W .

Case 3: R_J closed, R_I and B_J open. An unfolding for this case is depicted in Figure 27, which handles the case where JJ exists (handling the case where JJ does not exist requires only minor modifications).

First note that $\xrightarrow{e_A} \in R_I$ is open and adjacent to T_A , and \mathcal{N}_A provides a type-2 entry connection $\xrightarrow{e'_A} \in R_A$. Also note that $\xleftarrow{x'_A} \in L_A$ is closed and \mathcal{N}_A provides a type-1 exit connection $x'_A \in B_A$. These together show that \mathcal{N}_A satisfies invariant (I2). Since all open ring faces of A are used in entry and exit connections, \mathcal{N}_A trivially satisfies invariant (I3). The following observations support our claim that \mathcal{N}_A satisfies invariant (I1):

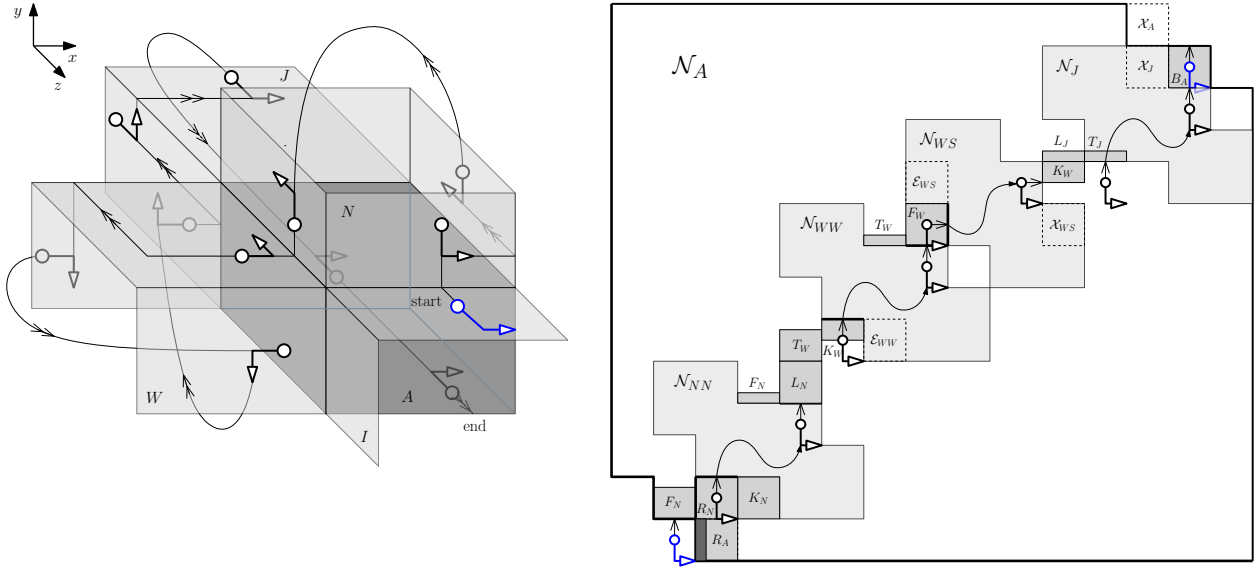


Figure 26: Unfolding of degree-4 box \$A\$ with \$N\$, \$W\$ and \$J\$ children (case \$R_J, R_I\$ closed).

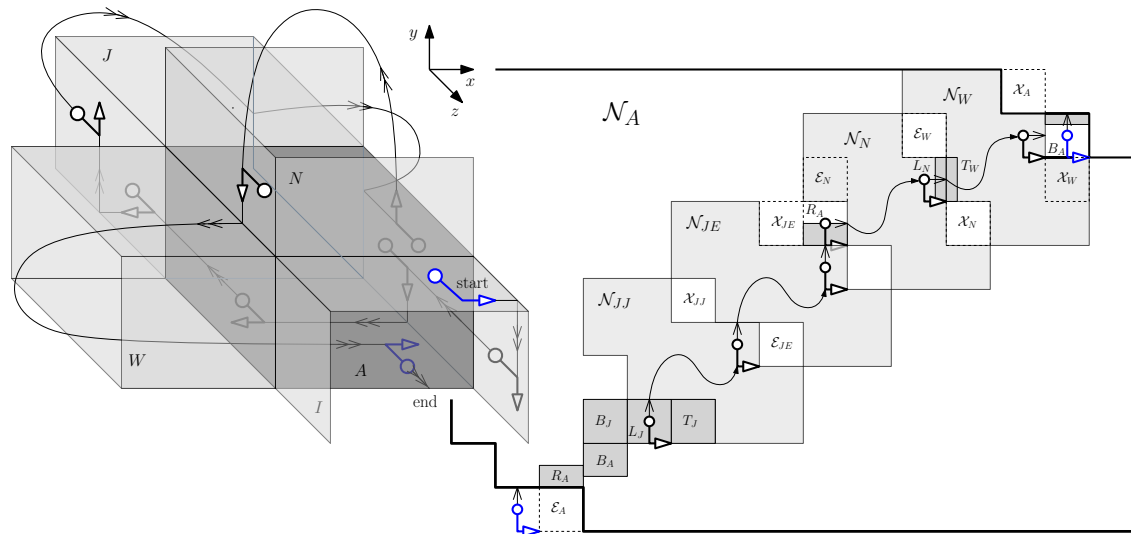


Figure 27: Unfolding of degree-4 box \$A\$ with \$N\$, \$W\$ and \$J\$ children (case \$R_J\$ closed, \$R_I\$ and \$B_J\$ open).

- The entry and exit ring faces for JJ , JE , N and W are as follows: $e_{JJ} \in L_J$ and $x_{JJ} \in K_{JE}$; $e_{JE} \in R_{JJ}$ and $x_{JE} \in R_A$; $e_N \in R_A$ and $x_N \in T_W$; and $e_W \in L_N$ (which connects to T_W) and $x_W \in B_A$.
- Since $\xrightarrow{e_{JJ}} \in T_J$ is open, the unit square \mathcal{E}_{JJ} (occupied by T_J in Figure 27) does not belong to the inductive region for JJ .
- \mathcal{N}_{JE} , \mathcal{N}_N and \mathcal{N}_W provide type-1 entry connections. This is because $\xrightarrow{e_{JE}} \in T_{JJ}$ is not adjacent to \mathcal{T}_{JE} , $\xrightarrow{e_N} \in F_A$ is closed, and $\xrightarrow{e_W} \in F_N$ is not adjacent to \mathcal{T}_W .
- \mathcal{N}_{JJ} , \mathcal{N}_{JE} , \mathcal{N}_N and \mathcal{N}_W provide type-1 exit connections. This is because $\xleftarrow{x_{JJ}} \in B_{JE}$ is not adjacent to \mathcal{T}_{JJ} , $\xleftarrow{x_{JE}} \in B_A$ is not adjacent to \mathcal{T}_{JE} , $\xleftarrow{x_N} \in K_W$ is not adjacent to \mathcal{T}_N , and $\xleftarrow{x_W} \in K_A$ is closed. Note that the type-1 exit connection of \mathcal{N}_{JJ} attaches to the type-1 entry connection of \mathcal{N}_{JE} , and the type-1 exit connection of \mathcal{N}_N attaches to the type-1 entry connection of \mathcal{N}_W .

Note that we split the unfolding of J into two subnets (\mathcal{N}_{JJ} and \mathcal{N}_{JE}) so as to avoid sharing the ring face $\xleftarrow{x'_J} \in B_J$ between its current position in \mathcal{N}_A (where it serves as a bridge between B_A and L_J) and the type-2 exit connection that \mathcal{N}_J would have provided (had it not been split).

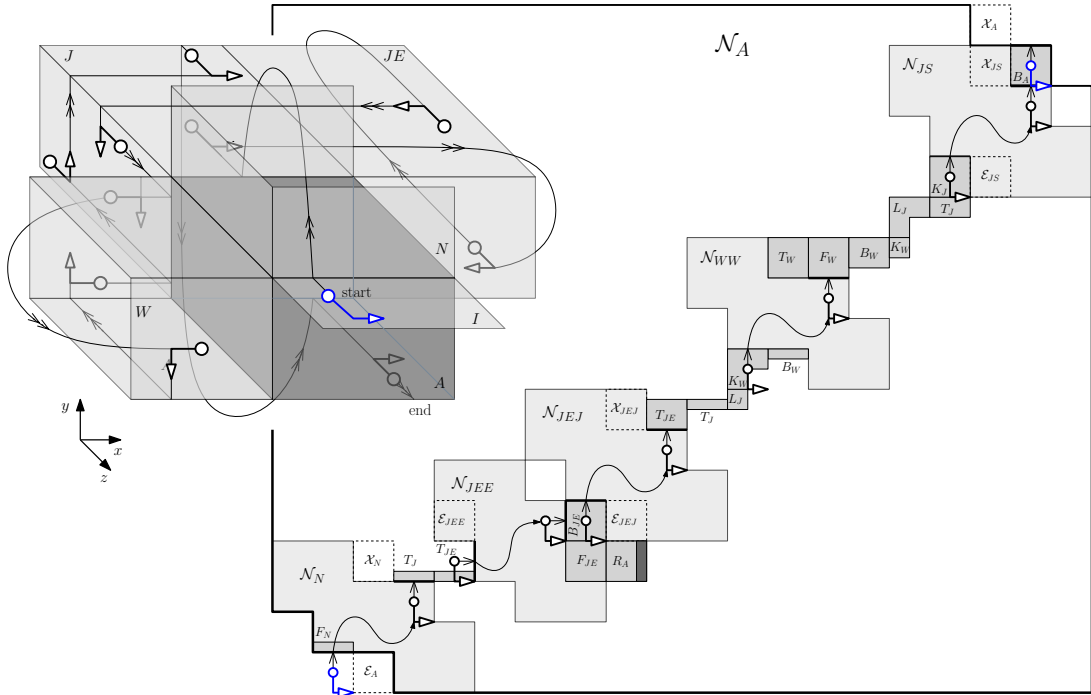


Figure 28: Unfolding of degree-4 box A with N , W and J children (case R_J closed, R_I open and B_J closed – so B_{JE} and B_W open); unfolding shown for the case when JEJ and JEE exist (so K_J open).

Case 4: R_J closed, R_I open and B_J closed. An unfolding for this case is depicted in Figure 28, which handles the more general case when JEJ and JEE exist. Arguments similar to the ones used in the proof of Case 1 of Lemma 19 show that the unfolding \mathcal{N}_A from Figure 28 satisfies invariants (I2) and (I3). The following observations support our claim that \mathcal{N}_A satisfies invariant (I1):

- The entry and exit ring faces for N , JEE , JEJ , WW and JS are as follows: $e_N \in T_I$ and $x_N \in T_J$; $e_{JEE} \in T_{JE}$ and $x_{JEE} \in B_{JE}$ (which is open, since B_J is closed); $e_{JEJ} \in B_{JE}$ and $x_{JEJ} \in T_{JE}$; $e_{WW} \in K_W$ and $x_{WW} \in F_W$; and $e_{JS} \in K_J$ (which is open, by our assumption that K_{JE} is closed) and $x_{JS} \in B_A$.

- \mathcal{N}_N , \mathcal{N}_{JEE} and \mathcal{N}_{JS} provide type-1 exit connections. This is because $\xleftarrow{x_N} \in L_J$ is not adjacent to \mathcal{T}_N , $\xleftarrow{x_{JEJ}} \in R_{JE}$ is closed (since JEE exists), and $\xleftarrow{x_{JS}} \in L_A$ is closed.
- Since $\xleftarrow{x_{JEE}} \in F_{JE}$ is open, the unit square \mathcal{X}_{JEE} (occupied by F_{JE} in Figure 28) does not belong to the inductive region for JEE .
- Since $\xrightarrow{e_{WW}} \in B_W$ and $\xleftarrow{x_{WW}} \in T_W$ are open, the unit squares \mathcal{E}_{WW} and \mathcal{X}_{WW} (occupied in Figure 28 by $\xrightarrow{e_{WW}}$ and T_W , respectively) do not belong to the inductive region for WW .
- \mathcal{N}_{JEE} , \mathcal{N}_{JEJ} and \mathcal{N}_{JS} provide type-1 entry connections. This is because $\xrightarrow{e_{JEE}} \in K_{JE}$ is closed (since JEJ exists), $\xrightarrow{e_{JEJ}} \in L_{JE}$ is closed, and $\xrightarrow{e_{JS}} \in R_J$ is closed. (Observe that the existence of JEJ implies that K_J is open.)

□

Lemma 22. Let $A \in \mathcal{T}$ be a degree-4 node with parent I and children N , E , and S (Case 4.5). If A 's children satisfy invariants (I1)-(I3), then A satisfies invariants (I1)-(I3).

Proof. The unfolding for this case involves three different case scenarios:

1. K_E open
2. K_E closed and L_I closed
3. K_E closed and L_I open

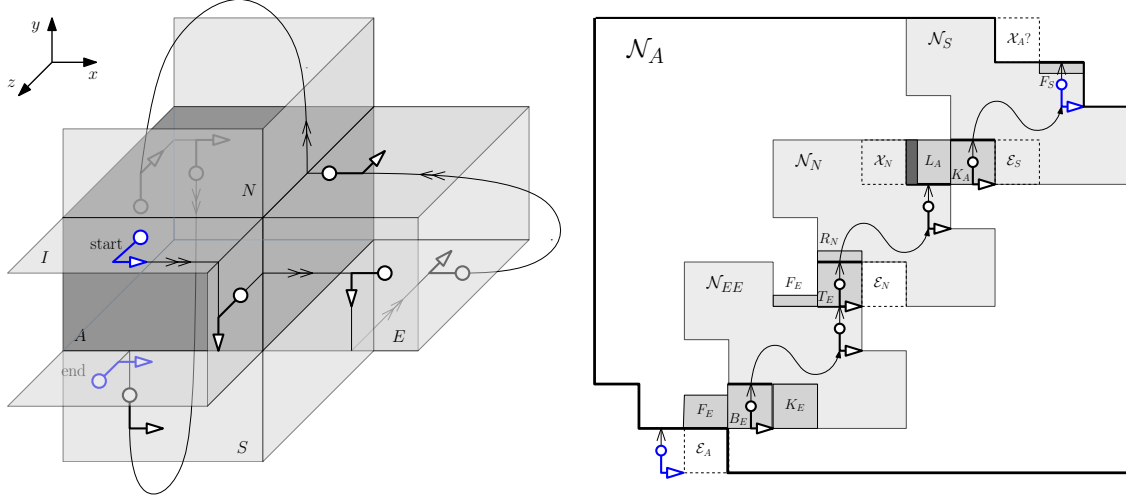


Figure 29: HAND-east unfolding of degree-4 box A with N , E and S children (case K_E open).

Case 1: K_E open. Note that in this case E is either a leaf or a connector. Consider the HAND-east unfolding depicted in Figure 29. Note that $\xrightarrow{e_A} \in R_I$ is open and adjacent to \mathcal{T}_A , and \mathcal{N}_A provides a type-2 entry connection $\xrightarrow{e'_A} \in F_E$. Also, since $\xleftarrow{x_S} \in L_I$ is not adjacent to \mathcal{T}_S , invariant (I2) applied to S tells us that \mathcal{N}_S provides a type-1 exit connection, which is also a type-1 exit connection for A (since $e'_A = e'_S \in F_S$). These together show that \mathcal{N}_A satisfies invariant (I2). The following observations support our claim that \mathcal{N}_A satisfies invariant (I1):

- The entry and exit ring faces for EE , N and S are as follows: $e_{EE} \in B_E$ and $x_{EE} \in T_E$; $e_N \in T_E$ and $x_N \in L_A$; and $e_S \in K_A$ and $x_S \in B_I$.
- Since $\xrightarrow{e_{EE}} \in K_E$ and $\xleftarrow{x_{EE}} \in F_E$ are open, the unit squares \mathcal{E}_{EE} and \mathcal{X}_{EE} (occupied in Figure 29 by K_E and $\xleftarrow{x_{EE}}$, respectively) do not belong to the inductive region for EE .

- \mathcal{N}_N provides type-1 entry and exit connections. This is because $\xrightarrow{e_N} \in K_E$ is not adjacent to \mathcal{T}_N (note however that it is open, so \mathcal{E}_N does not belong to the N 's inductive region), and $\xleftarrow{x_N} \in F_A$ is closed. Also \mathcal{N}_S provides a type-1 entry connection, since $\xrightarrow{e_S} \in R_A$ is closed.

Finally, observe that the ring face $\xrightarrow{x'} \in L_A$ (dark-shaded in Figure 29) can be removed from \mathcal{N}_A without disconnecting \mathcal{N}_A , so \mathcal{N}_A satisfies invariant (I3).

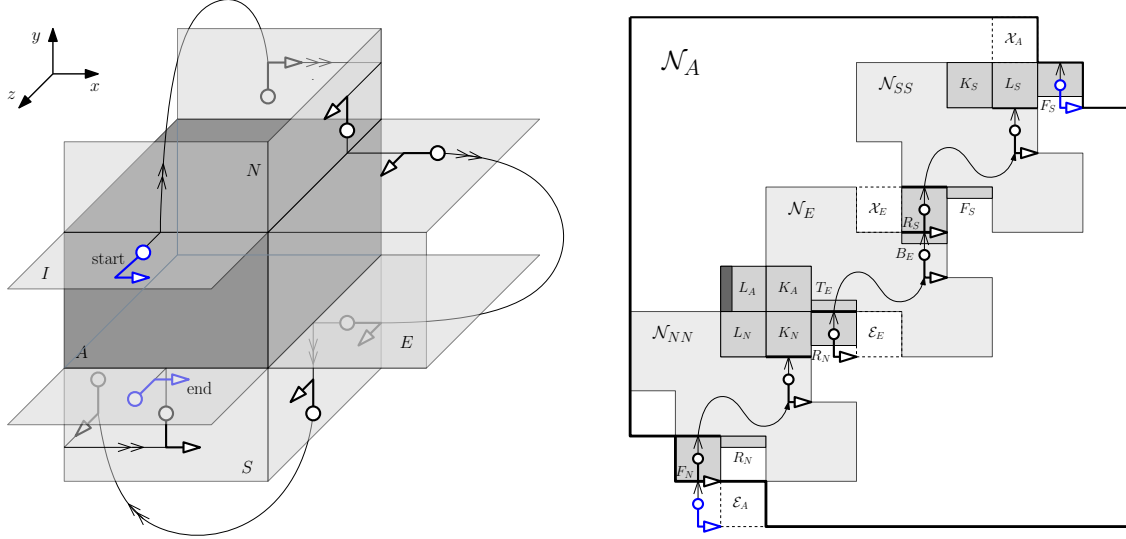


Figure 30: HAND-east unfolding of degree-4 box A with N , E and S children, case K_E closed (so K_N , K_S open) and L_I closed (so L_N , L_S open).

Case 2: K_E closed and L_I closed. Note that in this case K_N and K_S are open (since K_E is closed) and L_N and L_S are also open (since L_I is closed). Consider the HAND-east unfolding from Figure 30, and note that \mathcal{N}_A provides a type-1 entry connection $e'_A \in F_N$ and a type-1 exit connection $x'_A \in F_S$. Thus \mathcal{N}_A satisfies invariant (I2). The following observations support our claim that \mathcal{N}_A satisfies invariant (I1):

- The entry and exit ring faces for NN , E and SS are as follows: $e_{NN} \in F_N$ and $x_{NN} \in K_N$; $e_E \in R_N$ and $x_E \in R_S$; and $e_{SS} \in F_S$ and $x_{SS} \in L_S$.
- Since $\xrightarrow{e_{NN}} \in R_N$ and $\xleftarrow{x_{NN}} \in L_N$ are open, the unit squares \mathcal{E}_{NN} and \mathcal{X}_{NN} (occupied in Figure 30 by $\xrightarrow{e_{NN}}$ and L_N , respectively) do not belong to the inductive region for NN .
- Similarly, since $\xrightarrow{e_{SS}} \in F_S$ and $\xleftarrow{x_{SS}} \in K_S$ are open, the unit squares \mathcal{E}_{SS} and \mathcal{X}_{SS} (occupied in Figure 30 by $\xrightarrow{e_{SS}}$ and K_S , respectively) do not belong to the inductive region for SS .
- \mathcal{N}_E provides type-1 entry and exit connections, since $\xrightarrow{e_E} \in F_N$ and $\xleftarrow{x_E} \in K_S$ are not adjacent to \mathcal{T}_E .

Arguments similar to the ones above show that \mathcal{N}_A satisfies invariant (I3).

Case 3: K_E closed and L_I open. In this case we use $\xrightarrow{e_A} \in R_I$ and $\xleftarrow{x_A} \in L_I$ as entry and exit ring faces for the unfolding case when A has N , E and W children and K_E is closed. This approach is depicted in Figure 13, with the understanding that \mathcal{N}'_A is the net from Figure 21. Because $\xrightarrow{e_A} \in R_I$ and $\xleftarrow{x_A} \in L_I$ are both open and adjacent to \mathcal{T}_A , A may provide type-1 or type-2 entry and exit connections. Note that the unfolding net from Figure 21 provides a type-1 entry/exit connection, which is a type-2 entry/exit connection for \mathcal{N}_A . Since \mathcal{N}'_A satisfies invariants (I1)-(I3) (by Lemma 19), we conclude that \mathcal{N}_A satisfies invariants (I1)-(I3). \square

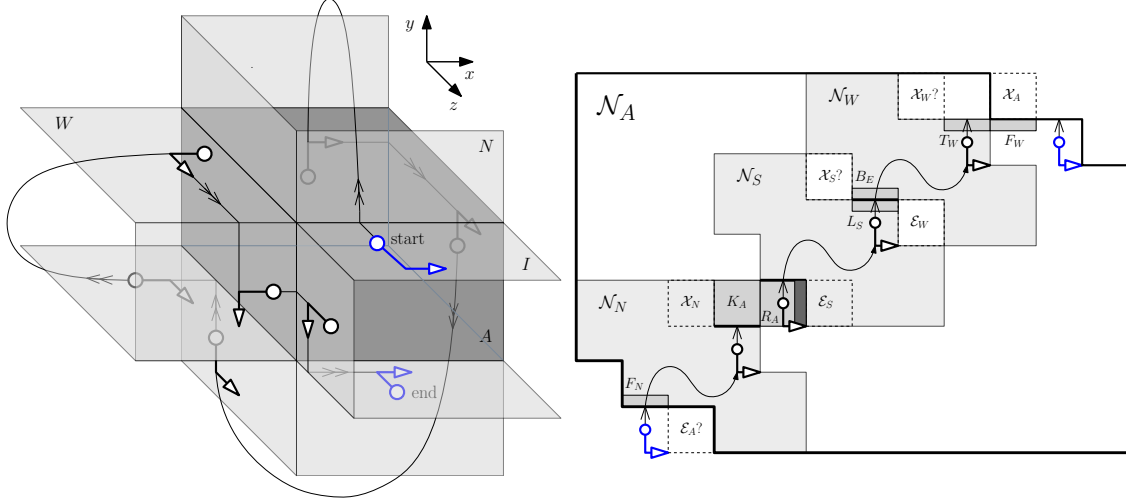


Figure 31: Unfolding of degree-4 box A with N , W and S children.

Lemma 23. Let $A \in \mathcal{T}$ be a degree-4 node with parent I and children N , W , and S (Case 4.6). If A 's children satisfy invariants (I1)-(I3), then A satisfies invariants (I1)-(I3).

Proof. Consider the unfolding from Figure 31, and notice that this is a general case of the degree-3 unfolding from Figure 18, where the unfolded face B_A is replaced by the recursive unfolding of child S . Arguments similar to the ones used in the proof of Case 1 of Lemma 17 show that the unfolding \mathcal{N}_A from Figure 31 satisfies invariants (I2) and (I3). Turning to (I1), note that \mathcal{N}_N , \mathcal{N}_S and \mathcal{N}_W all provide type-1 entry and exit connections. This is because $\xrightarrow{e_N} \in R_I$ is not adjacent to \mathcal{T}_N , $\xleftarrow{x_N} \in L_A$ and $\xrightarrow{e_S} \in F_A$ are closed, $\xleftarrow{x_S} \in K_W$ is not adjacent to \mathcal{T}_S , and $\xrightarrow{e_W} \in F_S$ and $\xleftarrow{x_W} \in K_N$ are not adjacent to \mathcal{T}_W . These together show that \mathcal{N}_A satisfies invariant (I1). \square

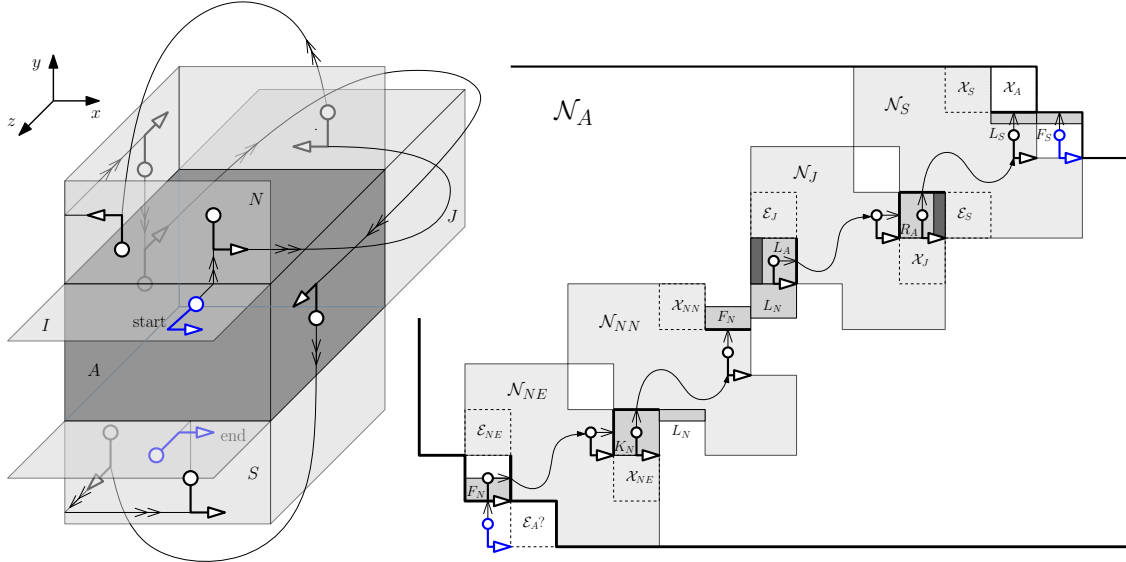


Figure 32: Unfolding of degree-4 box A with children N , J and S , case L_I closed (so L_N , L_S open); unfolding shown for the case when NN and NE exist.

Lemma 24. Let $A \in \mathcal{T}$ be a degree-4 node with parent I and children N , J , and S (Case 4.7). If A 's children satisfy invariants (I1)-(I3), then A satisfies invariants (I1)-(I3).

Proof. We discuss the following four exhaustive scenarios:

1. L_I and R_I open
2. L_I closed
3. R_I closed and L_J closed
4. R_I closed and L_J open

Case 1: L_I and R_I open. In this case I is a non-junction and we can use the unfolding from Figure 13, where we substitute \mathcal{N}'_A with the net from Figure 11. Because $\xrightarrow{e_A} \in R_I$ and $\xleftarrow{x_A} \in L_I$ are both open and adjacent to \mathcal{T}_A , \mathcal{N}_A may provide type-1 or type-2 entry and exit connections. Note that the unfolding net from Figure 11 provides a type-1 entry/exit connection, which is a type-2 entry/exit connection for \mathcal{N}_A . Since \mathcal{N}'_A satisfies invariants (I1)-(I3) (by Lemma 11), we conclude that \mathcal{N}_A satisfies invariants (I1)-(I3).

Case 2: L_I closed. Note that in this case L_N and L_S are open. Consider the unfolding from Figure 32, which handles the more general case when NN and NE exist (handling cases where one or both are missing requires only minor modifications). Note that \mathcal{N}_A provides a type-1 entry connection $e'_A \in F_N$ and a type-1 exit connection $x'_A \in F_S$, therefore \mathcal{N}_A satisfies invariant (I2). The following observations support our claim that \mathcal{N}_A satisfies invariant (I1):

- The entry and exit ring faces for NE , NN , J and S are as follows: $e_{NE} \in F_N$ and $x_{NE} \in K_N$; $e_{NN} \in K_N$ and $x_{NN} \in F_N$; $e_J \in L_A$ and $x_J \in R_A$; and $e_S \in R_A$ and $x_S \in L_A$.
- \mathcal{N}_{NE} , N_J and \mathcal{N}_S provide type-1 entry and exit connections. This is because $\xrightarrow{e_{NE}} \in T_N$ and $\xleftarrow{x_{NE}} \in B_N$ are closed (recall our assumption that NN exists), $\xrightarrow{e_J} \in B_A$ and $\xleftarrow{x_J} \in T_A$ are closed, and $\xrightarrow{e_S} \in F_A$ and $\xleftarrow{x_S} \in K_A$ are also closed.
- Since $\xrightarrow{e_{NN}} \in L_N$ is open, the unit square \mathcal{E}_{NN} (occupied by $\xrightarrow{e_{NN}}$ in Figure 32) does not belong to the inductive region for NN . Since $\xleftarrow{x_{NN}} \in R_N$ is closed, \mathcal{N}_{NN} provides a type-1 exit connection.

The two open ring faces of A not used in entry and exit connections are on L_A and R_A (dark-shaded in Figure 32), and they can be removed without disconnecting \mathcal{N}_A . It follows that \mathcal{N}_A satisfies invariant (I3). \square

Case 3: R_I and L_J closed. Note that in this case L_N and L_S are open, and the unfolding for this case is identical to the one shown in Figure 32.

Case 4: R_I closed and L_J open. Note that in this case R_N and R_S are open. Consider the unfolding from Figure 33, which handles the more general case when NN , NW , JE and JJ exist (handling cases when one or more of these boxes do not exist requires only minor modifications). Note that \mathcal{N}_A provides a type-1 entry connection $e'_A \in F_N$. Also note that $\xleftarrow{x_S} \in L_I$ is not adjacent to \mathcal{T}_S , therefore \mathcal{N}_S provides a type-1 exit connection, which is also a type-1 exit connection for \mathcal{N}_A (since $x_A = x_S$). These together show that \mathcal{N}_A satisfies invariant (I2). The following observations support our claim that \mathcal{N}_A satisfies invariant (I1):

- Since $\xrightarrow{e_A} \in R_I$ is closed, the unit square \mathcal{E}_A belongs to the inductive region of A .
- The entry and exit ring faces for NN , NW , JE , JJ and S are as follows: $e_{NN} \in K_N$ and $x_{NN} \in F_N$; $e_{NW} \in F_N$ and $x_{NW} \in K_N$; $e_{JE} \in T_J$ and $x_{JE} \in B_J$; $e_{JJ} \in B_J$ and $x_{JJ} \in T_J$; and $e_S \in B_J$ and $x_S \in B_I$.
- \mathcal{N}_{NN} , \mathcal{N}_{NW} , \mathcal{N}_{JE} and \mathcal{N}_S provide type-1 entry connections. This is because $\xrightarrow{e_{NN}} \in L_N$ is closed (since NW exists), $\xrightarrow{e_{NW}} \in B_N$ is closed, $\xrightarrow{e_{JE}} \in K_J$ is closed (since JJ exists), and $\xrightarrow{e_S} \in R_J$ is closed (since JE exists).
- Since $\xrightarrow{e_{JJ}} \in L_J$ is open, the unit square \mathcal{E}_{JJ} (occupied by $\xrightarrow{e_{JJ}}$ in Figure 33) does not belong to the inductive region for JJ .

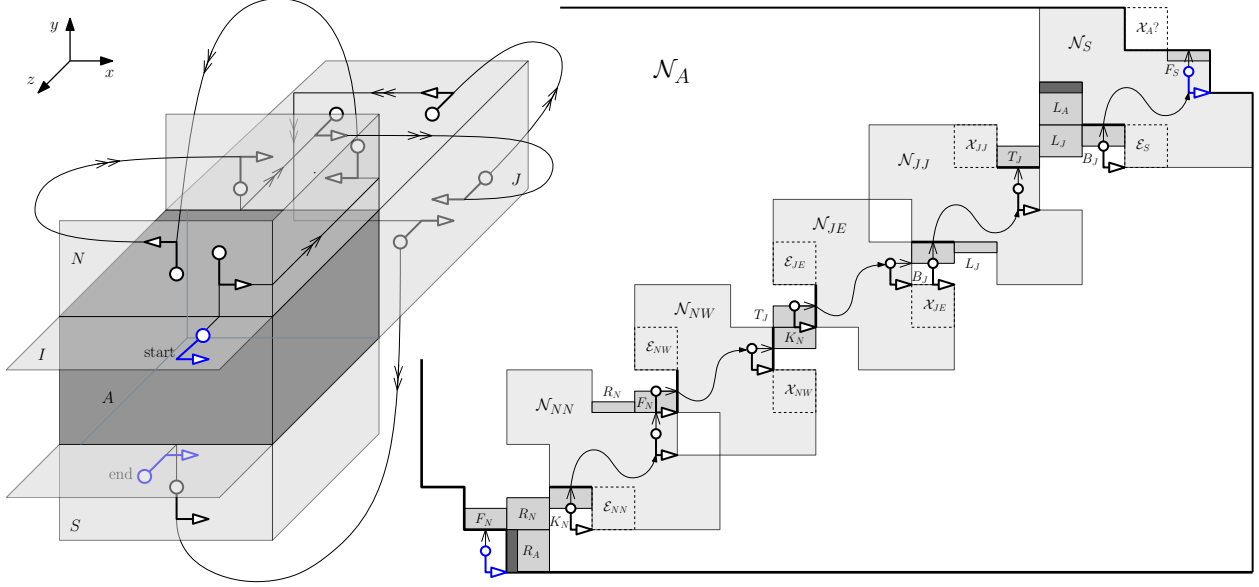


Figure 33: Unfolding of degree-4 box A with children N, J and S , case R_I closed (so R_N, R_S open) and L_J open; unfolding shown for the case when NN, NW, JE and JJ exist.

- Since $\xleftarrow{x_{NN}} \in R_N$ is open, the unit square \mathcal{X}_{NN} (occupied by $\xleftarrow{x_{NN}}$ in Figure 33) does not belong to the inductive region for NN .
- $\mathcal{N}_{NW}, \mathcal{N}_{JE}$ and \mathcal{N}_{JJ} provide type-1 exit connections. This is because $\xleftarrow{x_{NW}} \in T_N$ is closed (since NN exists), $\xleftarrow{x_{JE}} \in F_J$ is closed, and $\xleftarrow{x_{JJ}} \in R_J$ is closed (since JE exists).

Arguments similar to the ones used in the previous case show that \mathcal{N}_A satisfies invariant (I3) as well.

C Unfolding Degree-5 Nodes (Remaining Cases)

In this section we discuss the unfoldings for cases 5.2 through 5.4 listed in Section 7.4.

Lemma 25. *Let $A \in \mathcal{T}$ be a degree-5 node with parent I and children N, E, J and S (Case 5.2). If A 's children satisfy invariants (I1)-(I3), then A satisfies invariants (I1)-(I3).*

Proof. Arguments similar to the ones used in the proof of Lemma 12 show that either I and J are both non-junctions, or else N and S are both non-junctions.

The unfolding when I and J are both non-junctions is depicted in Figure 34. Note that this unfolding follows the same path as the one for the degree-4 case depicted in Figure 24, up to the point where it reaches L_J , where it slides to B_J to begin the recursive unfolding of S . Since these unfoldings and their correctness proofs are very similar, we only point out the differences here:

- Since $\xleftarrow{x_S} \in L_I$ is not adjacent to T_S , \mathcal{N}_S provides a type-1 exit connection $x'_S \in F_S$, which is also a type-1 exit connection for A .
- The ring face of J that lies on B_J is not used in \mathcal{N}_J 's entry and exit connection, therefore it can be relocated outside of \mathcal{N}_J (by invariant (I3) applied to J). We place it to the right of $x'_J \in L_J$ to serve as entry ring face for \mathcal{N}_S .
- Since $\xrightarrow{e_S} \in R_J$ is not adjacent to T_S , \mathcal{N}_S provides a type-1 entry connection $e'_S \in K_S$.

Assume now that N and S are both non-junctions. The unfolding for this case is depicted in Figure 35. Because $\xrightarrow{e_A} \in R_I$ is open and adjacent to T_A , \mathcal{N}_A has the option of providing a type-2 entry connection,

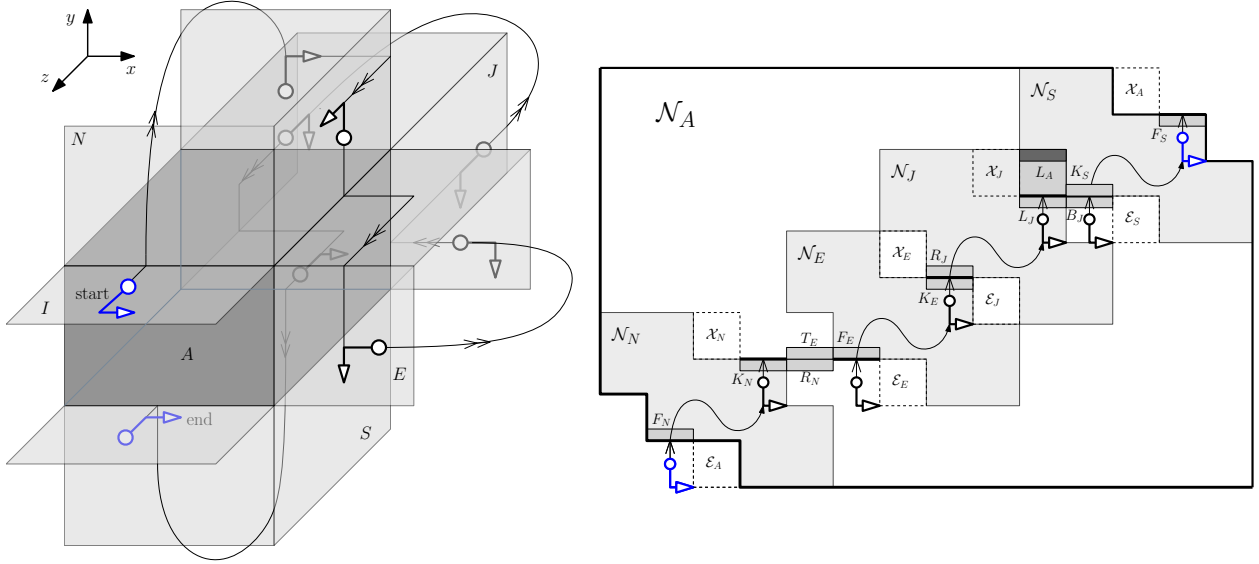


Figure 34: HANDEast unfolding of degree-5 box \$A\$ with \$N\$, \$E\$, \$J\$ and \$S\$ children, case when \$I\$ and \$J\$ are both non-junctions.

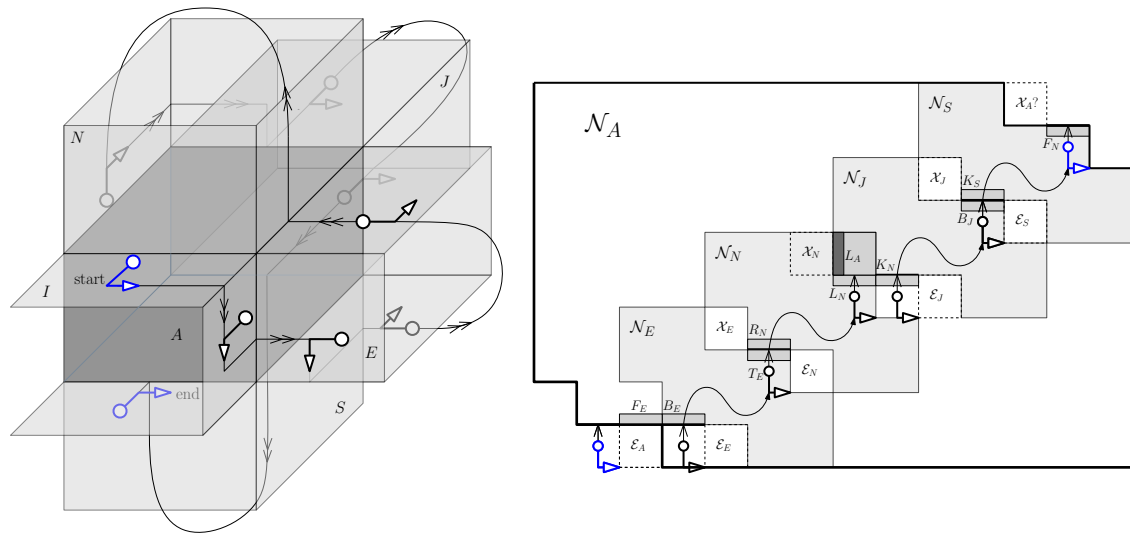


Figure 35: HANDEast unfolding of degree-5 box \$A\$ with \$N\$, \$E\$, \$J\$ and \$S\$ children, case when \$N\$ and \$S\$ are both non-junctions.

which it does by placing $\xrightarrow{e'_A} \in F_E$ adjacent to the entry port extension. It also provides a type-1 exit connection $x'_A = x'_S \in F_S$, and therefore \mathcal{N}_A satisfies invariant (I2). Also note that (I3) is satisfied, since A 's ring face on L_A (darkened in Figure 35) is not used in entry or exit connections and can be removed without disconnecting \mathcal{N}_A . The following observations support our claim that \mathcal{N}_A is connected and satisfies invariant (I1):

- The entry and exit ring faces for E , N , J and S are as follows: $e_E \in R_S$ and $x_E \in R_N$; $e_N \in T_E$ and $x_N \in L_A$; $e_J \in K_N$ and $x_J \in K_S$; and $e_S \in B_J$ and $x_S \in B_I$.
- All children nets provide type-1 entry connections (by invariant (I2)). This is because $\xrightarrow{e_E} \in K_S$ is not adjacent to \mathcal{T}_E , $\xrightarrow{e_N} \in K_E$ is not adjacent to \mathcal{T}_N , $\xrightarrow{e_J} \in R_N$ is not adjacent to \mathcal{T}_J , and $\xrightarrow{e_S} \in R_J$ is not adjacent to \mathcal{T}_S . In addition, all children provide type-1 exit connections because $\xleftarrow{x_E} \in F_N$ is not adjacent to \mathcal{T}_E , $\xleftarrow{x_N} \in F_A$ is closed, $\xleftarrow{x_J} \in L_S$ is not adjacent to \mathcal{T}_J , and $\xleftarrow{x_S} \in L_I$ is not adjacent to \mathcal{T}_S .
- Ring faces that lie on F_E and K_N can be relocated anywhere outside of \mathcal{N}_E and \mathcal{N}_N respectively, by invariant (I3), noting that none of these ring faces are used in any entry or exit connections.
- The exit connection $x'_N \in L_N$, because N is a non-junction and L_N is open. Thus L_A is attached to $x'_N \in L_N$ in the unfolding.

This concludes the proof. \square

Lemma 26. *Let $A \in \mathcal{T}$ be a degree-5 node with parent I and children N , W , J and S (Case 5.3). If A 's children satisfy invariants (I1)-(I3), then A satisfies invariants (I1)-(I3).*

Proof. Arguments similar to the ones used in the proof of Lemma 12 show that either I and J are both non-junctions, or else N and S are both non-junctions.

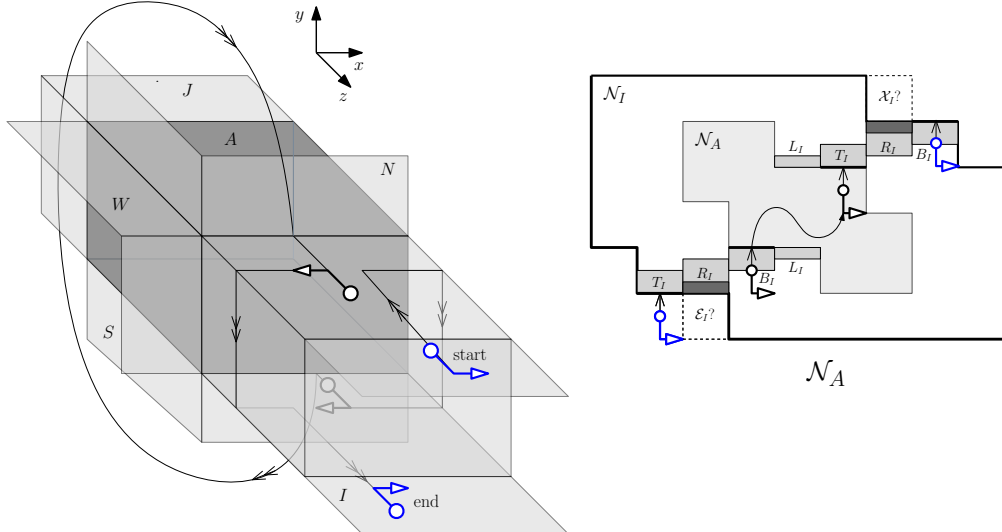


Figure 36: Unfolding of degree-5 box A with N , W , J and S children, case when I and J are both non-junctions.

The unfolding for the case when I and J are both non-junctions can be reduced to the case from Figure 34 using the method depicted in Figure 36. In this case, I 's unfolding is handled specially, so we describe the recursive unfolding of I assuming I is in standard position (with A in the back). The unfolding path starts at the top front edge of I and cycles clockwise to I 's bottom back edge, which is A 's entry port. By using this bottom entry port, A 's unfolding is a horizontal reflection of that in Figure 34. After unfolding A , the unfolding path cycles counter-clockwise from the top back edge of I (which is A 's exit port) to I 's bottom front edge.

Observe in the unfolding shown in Figure 36 that \mathcal{N}_I provides type-1 entry and exit connections, I 's ring faces not used in entry or exit connections (shown darkened) can be removed without disconnecting \mathcal{N}_I , and all open faces of I are unfolded. We have already established that \mathcal{N}_A satisfies invariants (I1)-(I3) and provides type-1 entry and exit connections, which connect to the pieces B_I and T_I placed adjacent to them. Thus \mathcal{N}_I satisfies invariants (II)-(I3).

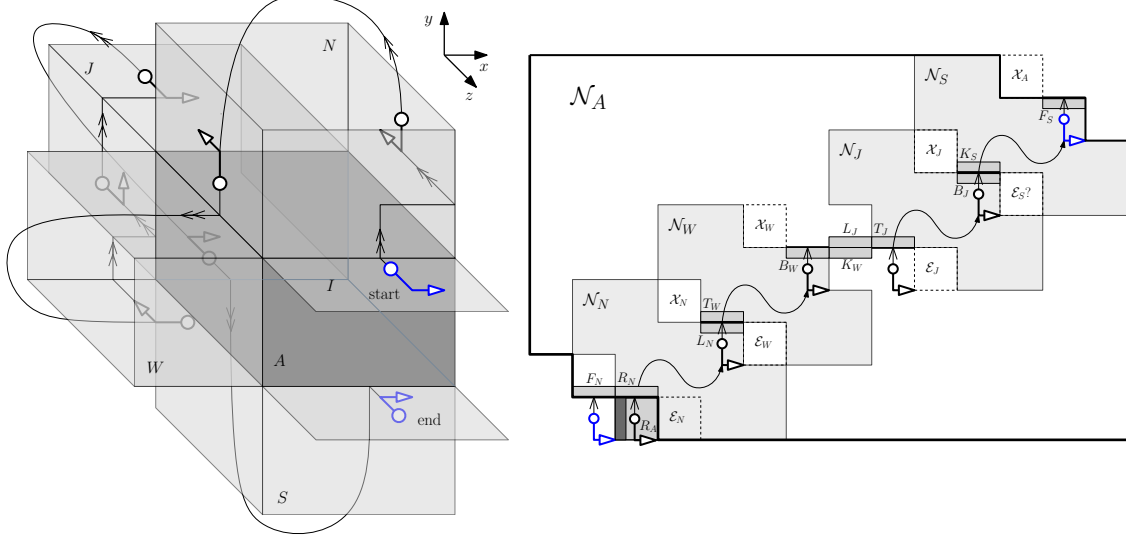


Figure 37: Unfolding of degree-5 box A with N , W , J and S children, case when N and S are both non-junctions and I has an east neighbor.

Consider now the case when N and S are both non-junctions. If I has a neighbor to its east, then the unfolding is as depicted in Figure 37. The net \mathcal{N}_A provides a type-1 entry connection $e'_A \in F_N$ and a type-1 exit connection $x'_A = x'_S \in F_S$. Therefore \mathcal{N}_A satisfies invariant (I2). Also note that (I3) is satisfied, since A 's ring face on R_A (darkened in Figure 37) is not used in entry or exit connections and can be removed without disconnecting \mathcal{N}_A . Because R_I is closed, \mathcal{E}_A is part of \mathcal{N}_A 's inductive region and therefore the face R_A can be placed there. The following observations support our claim that \mathcal{N}_A is connected and satisfies invariant (I1):

- The entry and exit ring faces for N , W , J and S are as follows: $e_N \in R_A$ and $x_N \in T_W$; $e_W \in L_N$ and $x_W \in L_S$; $e_J \in K_N$ and $x_J \in K_S$; and $e_S \in B_J$ and $x_S \in B_I$.
- All children nets provide type-1 entry connections (by invariant (I2)). This is because $\xrightarrow{e_N} \in K_A$ is closed, $\xrightarrow{e_W} \in K_N$ is not adjacent to T_W , $\xrightarrow{e_J} \in R_N$ is not adjacent to T_J , and $\xrightarrow{e_S} \in R_J$ is not adjacent to T_S . In addition, all children provide type-1 exit connections because $\xleftarrow{x_N} \in F_W$ is not adjacent to T_N , $\xleftarrow{x_W} \in F_S$ is not adjacent to T_W , $\xleftarrow{x_J} \in L_S$ is not adjacent to T_J , and $\xleftarrow{x_S} \in L_I$ is not adjacent to T_S .
- Ring faces that lie on F_N , L_J and K_W can be relocated anywhere outside of \mathcal{N}_N , \mathcal{N}_J and \mathcal{N}_W respectively, by invariant (I3), noting that none of these ring faces are used in any entry or exit connections.

If I does not have a neighbor to its west, then I is a non-junction and the unfolding can be reduced to the case depicted in Figure 35 using the technique outlined in Figure 36: the path cycles around I to B_I and A is unfolded using a horizontal reflection of Figure 35. The proof that this satisfies invariants (I1)-(I3) is similar to the one used for the unfolding in Figure 36, noting that here \mathcal{N}_A has a type-2 entry connection that attaches to L_I in Figure 36. \square

Lemma 27. *Let $A \in \mathcal{T}$ be a degree-5 node with parent I and children E , W , J and S (Case 5.4). If A 's children satisfy invariants (I1)-(I3), then A satisfies invariants (I1)-(I3).*

Proof. Arguments similar to the ones used in the proof of Lemma 12 show that either E and W are both non-junctions, or else I and J are both non-junctions.

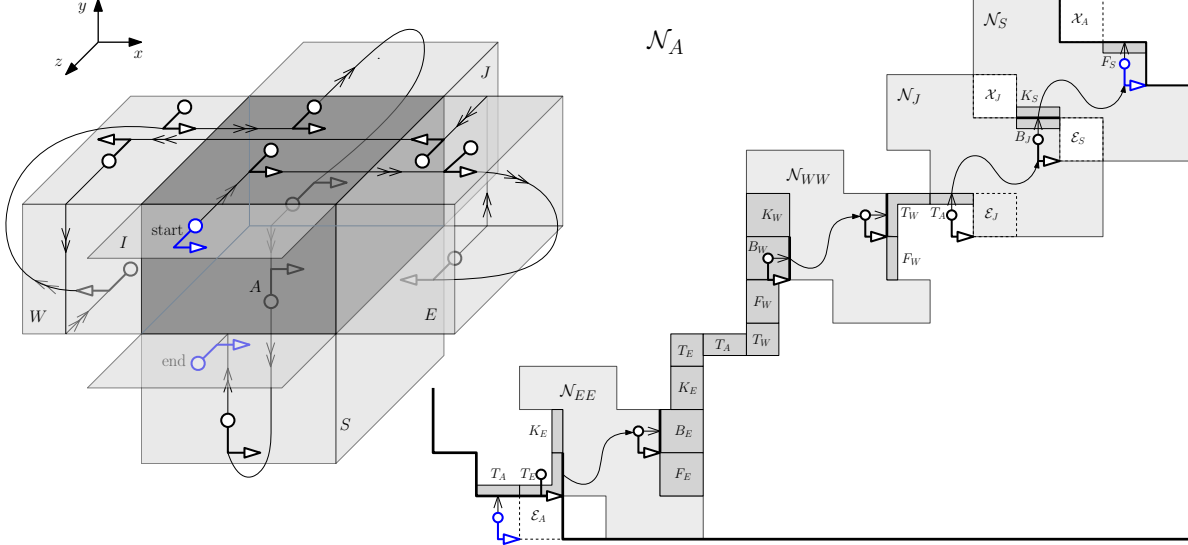


Figure 38: Unfolding for box A of degree 5 with E , W , J and S children, case when E and W are both non-junctions.

The unfolding for the case when E and W are both non-junctions is depicted in Figure 38. Note that \mathcal{N}_A provides a type-1 entry connection $e'_A \in T_A$ and a type-1 exit connection $x'_A \in F_S$, therefore \mathcal{N}_A satisfies invariant (I2). Also note that (I3) is trivially satisfied, since A has a single open ring face $e'_A \in T_A$ that is an entry connection. The following observations support our claim that \mathcal{N}_A is connected and satisfies invariant (I1):

- The entry and exit ring faces for EE , WW , J and S are as follows: $e_{EE} \in T_E$ and $x_{EE} \in B_E$; $e_{WW} \in B_W$ and $x_{WW} \in T_W$; $e_J \in T_A$ and $x_J \in K_S$; and $e_S \in B_J$ and $x_S \in B_I$.
- \mathcal{N}_J and \mathcal{N}_S provide type-1 entry and exit connections. This is because $\xrightarrow{e_J} \in R_A$ is closed, $\xleftarrow{x_J} \in L_S$ is not adjacent to T_J , and $\xrightarrow{e_S} \in R_J$ and $\xleftarrow{x_S} \in L_I$ are open but not adjacent to T_S .
- Since $\xrightarrow{e_{EE}} \in K_E$ and $\xleftarrow{x_{EE}} \in F_E$ are open, the unit squares \mathcal{E}_{EE} and \mathcal{X}_{EE} (occupied in Figure 38 by $\xrightarrow{e_{EE}}$ and F_E , respectively) do not belong to the inductive region for EE .
- Since $\xrightarrow{e_{WW}} \in K_W$ and $\xleftarrow{x_{WW}} \in F_W$ are open, the unit squares \mathcal{E}_{WW} and \mathcal{X}_{WW} (occupied in Figure 38 by K_W and $\xleftarrow{x_{WW}}$, respectively) do not belong to the inductive region for WW .

If I and J are non-junctions, then we use the unfolding from Figure 13, with the understanding that \mathcal{N}'_A is the net from Figure 34. Note that \mathcal{N}'_A provides type-1 entry and exit connections, which implies that the net \mathcal{N}_A from Figure 13 provides type-2 entry and exit connections. Since $\xrightarrow{e_A} \in R_I$ and $\xleftarrow{x_A} \in L_I$ are open and adjacent to T_A , and \mathcal{N}'_A satisfies invariants (I1)-(I3), we conclude that \mathcal{N}_A satisfies invariants (I1)-(I3). \square

D Another Complete Unfolding Example

We conclude this paper with another complete unfolding example that incorporates some of the cases presented in the appendices (which could not be included in the first example from Section 8). We use as running example a polycube tree composed of nine boxes, depicted in Figure 39. The root A of the the unfolding tree is a degree-1 box with back child J , which is unfolded recursively. The unfolding of J follows the pattern depicted in Figure 17b, slightly adjusted to accommodate for the fact that J does not have a south-east child. The east-east child of J (labeled C in Figure 39) follows the unfolding pattern depicted in Figure 7a. The

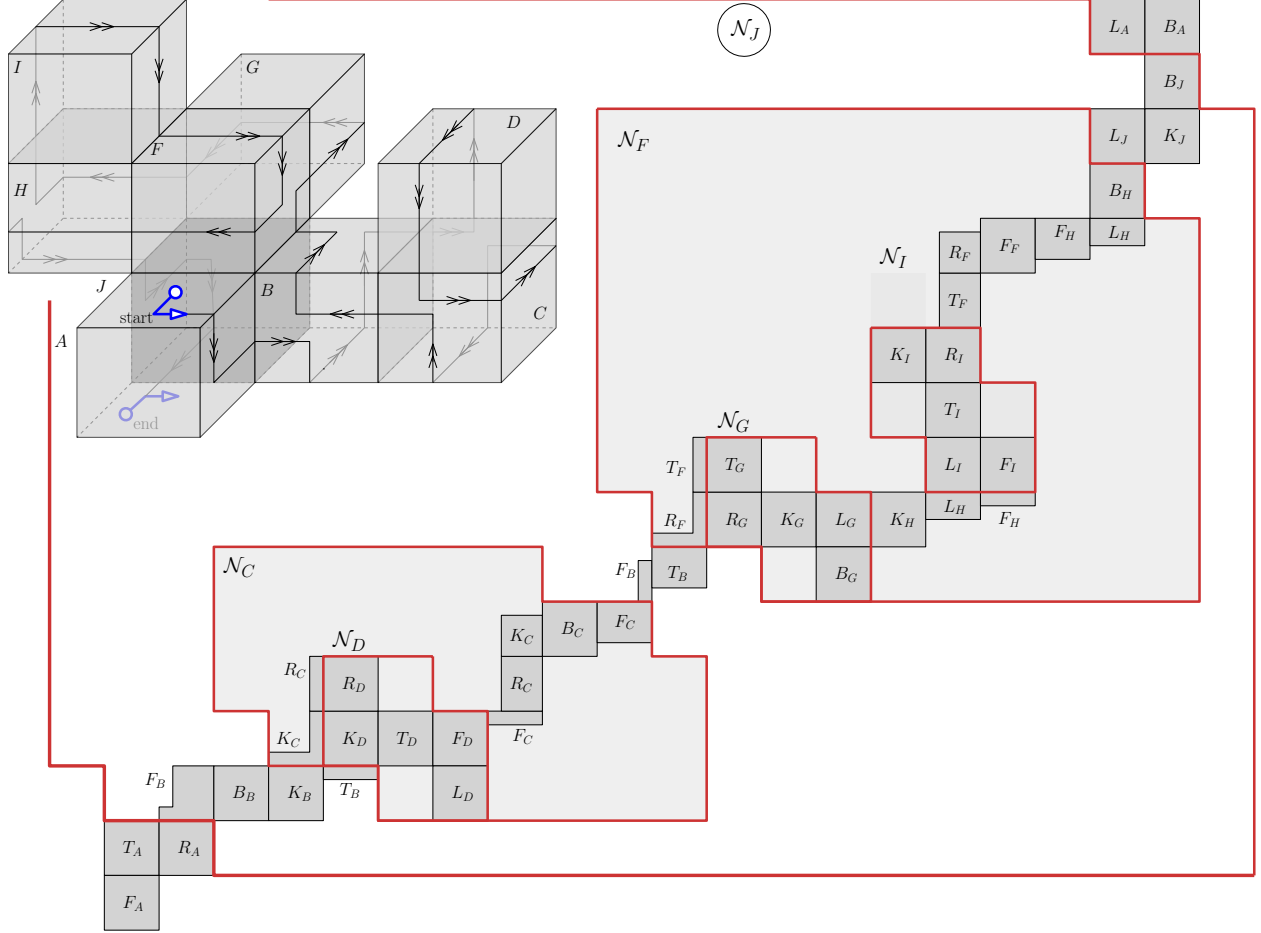


Figure 39: Unfolding of polycube tree with root A (back child of A is J).

north child of J (labeled F in Figure 39) follows the unfolding pattern from Figure 18b, traversed on reverse (note that the subtree rooted at F is a horizontal mirror plane reflection of the case depicted in Figure 18b, after a clockwise 90° -rotation about a vertical axis followed by a clockwise 90° -rotation about a horizontal axis, to bring it in standard position). Finally, the leaves are unfolded as in Figure 2.